Alteration of hyaloclastites in the HSDP 2 Phase 1 Drill Core 1. Description and paragenesis

Anthony W. Walton

Department of Geology, University of Kansas, 1475 Jayhawk Boulevard, Lawrence, Kansas 66045, USA (Twalton@ku.edu)

Peter Schiffman

Department of Geology, University of California, Davis, 1 Shields Boulevard, Davis, California 95616, USA

[1] The core from the Hawaii Scientific Drilling Project 2 Phase 1 provides a unique opportunity for studying the low-temperature alteration processes affecting basalt in suboceanic-island environments. In hyaloclastites, which make up about one half of the lower 2 km of this core (the portion that accumulated below sea level), these processes have resulted in zones of incipient, smectitic, and palagonitic alteration. The alteration of sideromelane in these hyaloclastites has four distinct outcomes: dissolution, replacement by two different textural varieties of smectite (i.e., reddened and green grain-replacive), and conversion to palagonite. All samples show evidence of the incipient stage of alteration, suggesting that every sample passed through that zone. However, most samples that show palagonitic alteration do not also show evidence of smectitic alteration and vice versa, suggesting these two outcomes represent divergent paths of alteration. Incipient alteration (1080 to 1335 m depth) includes fracturing and mechanical reduction of porosity from 40–45% to about 20–30%; growth of one form of pore-lining smectite; dissolution of sideromelane; and formation of sideromelane-grain replacements consisting of Fe-hydroxide-strained smectite, titaniferous nodules, and tubules. DNA-specific stains and morphological features indicate that tubules are the result of microbial activity. Smectitic alteration (1405 to 1573 m) includes growth of a second variety of pore-lining smectite, pore-filling and grain-replacing smectite, and cements of phillipsite and Ca-silicate minerals. Palagonitic alteration (1573 m to the deepest samples) includes replacement of margins of shards with palagonite and growth of pore-filling chabazite. The porosity is reduced by cementation to less than 4% at 1573 m. Porosity does not decrease further down hole, nor does the thickness of palagonite rims on shards increase through the zone of palagonitic alteration. In these samples, palagonite is not an intermediate alteration product in the development of smectite. Rather, in hyaloclastites from the HSDP core, palagonite has formed after all observed smectites. Current downhole temperatures at the boundaries between the three alteration zones are in the range from 12° to 15°C, suggesting that geochemical thresholds or vital effects, not temperature conditions, control different outcomes of alteration.

1. Introduction

[2] The HSDP 2 Phase 1 drilling program recovered some 95% of the core drilled from a 3.06 km-deep hole on the south east flank of Mauna Loa volcano (Hawaii Scientific Drilling Project-2, 2000; referred to subsequently as HSDP-2). From approximately 1080 mbsl to the bottom, the core contained submarine lithologies including hyaloclastite and pillowed or massive lavas with minor intrusive basalts (Figure 1). Hyaloclastite is the dominant lithology in the upper half of this submarine section and is subordinate to pillow lavas in the lower half. Over the submarine portion of the core, approximately half of the section was initially described as hyaloclastite [*DePaolo et al.*, 2000].

[3] This contribution describes the features of alteration of the hyaloclastites encountered in Phase I of the HSPD 2 boring. It emphasizes identification of phases, petrographic description of textures and sequence of events, and comparison to other palagonite-bearing successions. This description was undertaken as a preliminary step in attempting to understand the mass balance and processes of alteration of the rocks in the borehole.

1.1. Palagonite

[4] Palagonite (palagonit of *von Waltershausen* [1845], as reported by *Peacock* [1926]) is an alteration product of sideromelane, the variety of basalt glass that contains few quench crystals and appears transparent and light colored in thin section. Reviews by *Honnorez* [1981], *Fisher and Schmincke* [1984], *Singer and Banin* [1990], and *Stroncik and Schmincke* [2001] summarize the considerable literature on usage of the term palagonite, formation of palagonite, and chemical changes in forming palagonite. We follow *Stroncik and Schmincke* [2001] and widespread usage in applying the term palagonite to gel-like material that replaces sideromelane (Figure 2). Palagonite is

yellow-orange in plane polarized light, isotropic or very nearly so, and may include internal layering or banding shown by inclusions or color.

[5] *Peacock* [1926] described gel-palagonite and fibro-palagonite as different forms of palagonite. Fibro-palagonite, while it occurs as a replacement of sideromelane, has been identified as smectite, perhaps poorly crystalline smectite [*Zhou et al.*, 1992]. Hence *Stroncik and Schmincke* [2001] follow many other authors and recommend that fibro-palagonite not be used and what has been called gel palagonite simply be called palagonite. *Honnorez* [1981] went further, suggesting abandoning the term palagonite all together while retaining the term palagonitization to describe the alteration of sideromelane. It seems misleading to us to describe the diversity of outcomes of the alteration process of sideromelane by one term. Four such processes are described here. Instead, we view palagonitization as the process of forming palagonite.

2. Techniques

[6] This study draws heavily upon petrographic description. It employed standard thin sections that were prepared after samples were impregnated with blue-dyed epoxy to make pores visible. Descriptions of the thin sections included mineralogy and relative age relationships of phases. Point counts include about 150 points in standard thin sections, the number limited by the coarse size of grains. This means that the precision of values is low [*van der Plas and Tobi*, 1965].

[7] X-ray diffraction studies of thin sections and powdered fragments separated from samples, electron microprobe chemical analysis, and examination by scanning electron microscope supplemented visual mineral identifications and petrographic textural description. X-ray diffraction used a Rigaku X-ray diffractometer with Cu Kα radiation. Sam-
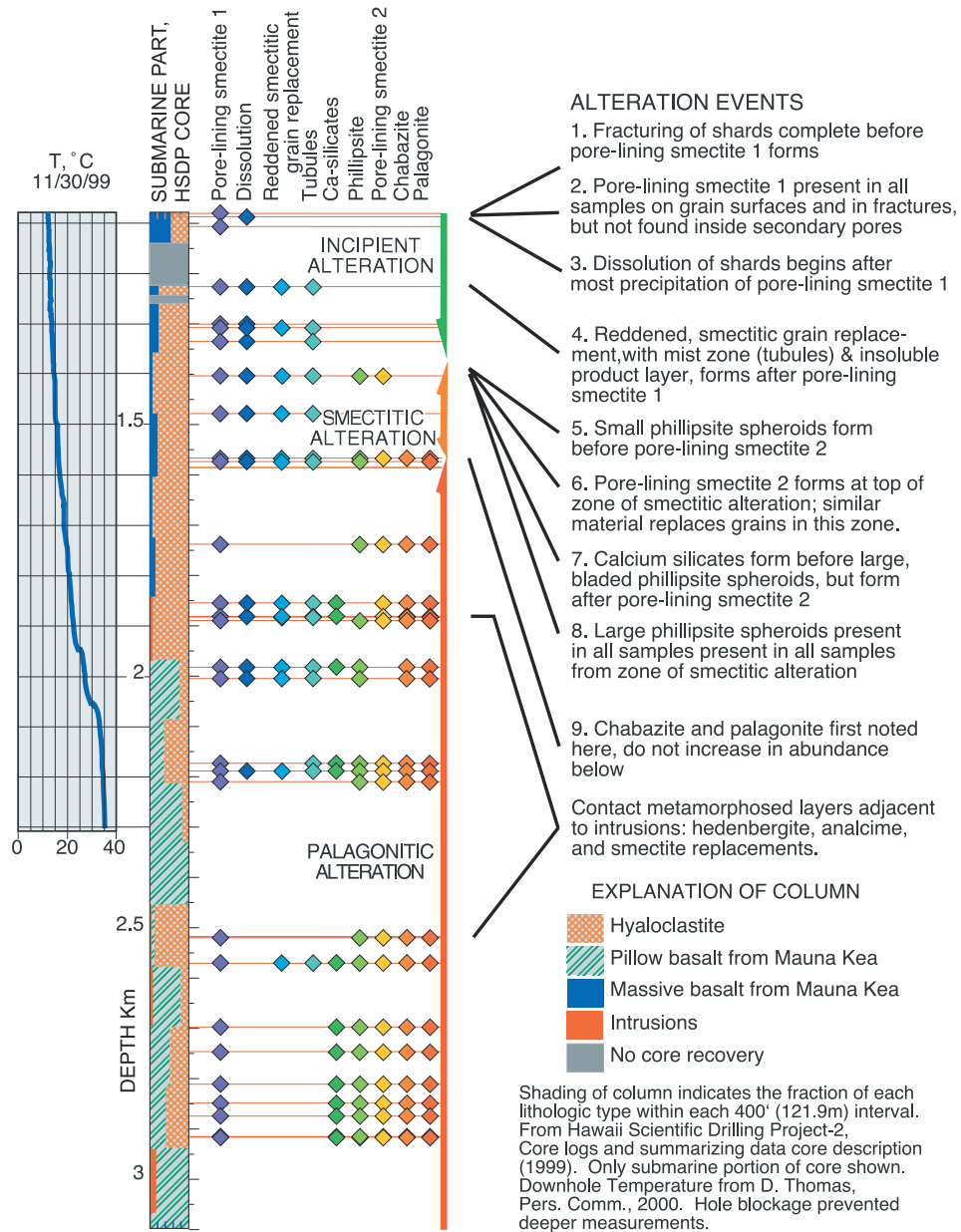
Figure 1. Summary of alteration of hyaloclastites in the submarine portion of the core from HSDP 2 Phase 1. Distribution of phases allows definition of different zones. Textures and phases formed in zone of incipient alteration remain present to the bottom of the core. Core description is modified from Hawaii Scientific Drilling Project-2 (2000). Temperature log is latest available. The upper 1.08 km pertaining to the subaerial portion of the core is omitted from both the lithologic column and temperature log, and the latter does not extend to bottom of hole because of blockage.

ples were either whole (uncovered) thin sections or mineral separates from thin sections or hand specimens that were powdered and mounted on glass slides. Compositional analyses of minerals, glass, and palagonite were conducted by wavelength dispersive spectrometry using a Cameca SX-50 electron microprobe operated at 15 KeV, 5–10 nA beam current, and using a rastered, defocused beam. The microprobe was also used for backscattered electron (BSE) imaging.

[8] Some samples, including some containing villiform tubules, were stained with DAPI (4′, 6-diamidino-2-phenylindole), to test whether the tubules have a microbial origin [*Furnes et al.*, 1996]. Although the procedure was developed for
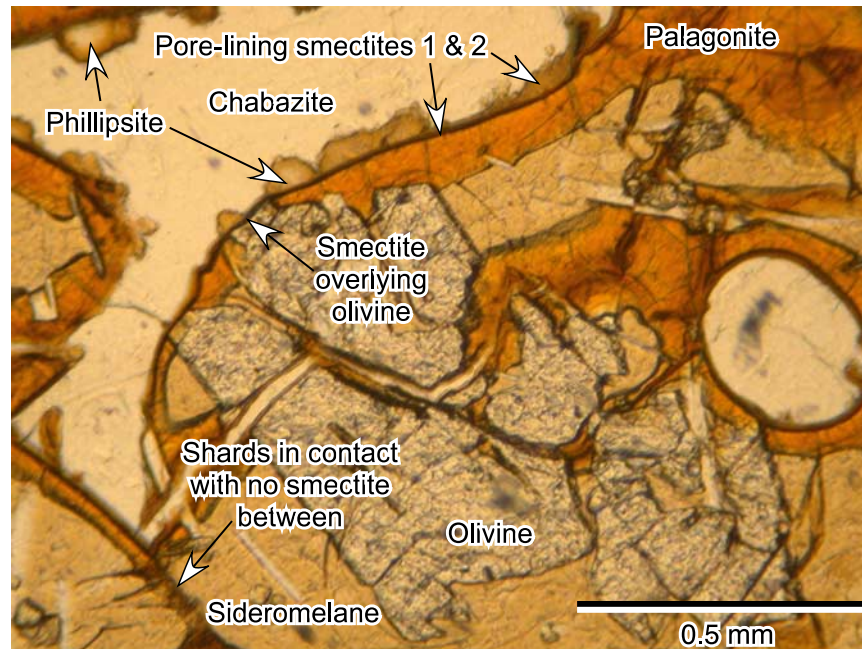
Figure 2. Palagonitic alteration in a hyaloclastite from HSDP 1 Phase 1 core (2565.7 m depth). Hyaloclastite shards were fractured, then coated with brown pore-lining smectite 1. Note that smectite coating is present where the olivine grain forms the margin of the large shard (top center), but is missing in lower left where two shards are in contact. After formation of fibrous spherulites of phillipsite, green pore-lining smectite 2 formed. The last stage of alteration included forming palagonite margins on shards (yellow-orange) and pore-filling chabazite. Sample is imaged in plane-polarized light.

staining DNA in bacteria on filters, experiments indicate that it is satisfactory for staining DNA in thin sections [*Yu et al.*, 1995; J. R. Rogers, personal communication, 2002]. DAPI-stained samples were imaged on a Nikon E600 microscope equipped with epifluorescence and phase contrast.

3. Hyaloclastite, Sideromelane, and Alteration Products

[9] The HSDP 2 phase 1 core sampled a large number of different lithologic units. This study considers hyaloclastites, as described in the initial report from the project [*DePaolo et al.*, 2000]. The samples we studied are all believed to come from eruptions of Mauna Kea or satellite vents of that volcano. Sample depths and some petrographic information are included in Table 1.

3.1. Hyaloclastite and Sideromelane

[10] Hyaloclastites consist of angular fragments and shards ranging from less than 0.1 mm greatest

diameter to decimeter scale (or perhaps larger). Fragments contain phenocrysts, various concentrations of quench crystallites, and basalt glass or sideromelane. Sideromelane is dark brown, dark green or nearly black in hand specimen, but is pale tan and isotropic in thin section (Figures 2, 3, and 4). Macroscopically, most hyaloclastite intervals are not obviously sorted and not bedded. Some intervals, however, are distinctly laminated or bedded, probably as the result of re-sedimentation processes after original emplacement [*DePaolo et al.*, 2000].

[11] Sideromelane in hyaloclastites ranges from completely fresh to completely altered. Alteration of hyaloclastite shards includes fracturing, conversion to palagonite, smectitic replacement, and dissolution. Tubules are prominent features of sideromelane (or palagonite that replaces it) in many, but not all, samples. Several varieties of smectite, zeolites, Ca-silicates, and other minerals have formed in both primary and secondary pores. Most olivine and plagioclase phenocrysts in hya-

Table 1. Hyaloclastite Samples Examined During This Study[a]

Run and dist. below run top, ft	Subsea depth, ft (m)	Lithology	Alteration	Tubules	Alteration features
R 0447 9.7 to 9.8	3540.8 (1079.2)	Tachylite clasts. Uppermost described hyaloclastite	Incipient	None observed	Minor smectite in olivine. Brown, nearly isotropic isopachous pore linings (smectite I?)
R0451 5.8	3567.4 (1087.3)	Hyaloclastite w. porphyritic diabase clasts	Incipient	None observed	Minor dissolution of sideromelane
R0459 3	3631.1 (1106.8)	Hyaloclastite	Incipient	None observed	Very thin, faintly birefringent grain coatings
R0466 1.1 to 1.2	4022.2 (1226.0)	Hyaloclastite	Incipient	Tubules in some areas, short and straight.	Isopachous to spherulitic smectite, substantial dissolution of sideromelane. Titaniferous nodules in dissolved pores. Some RSGR with mist zone.
R0514 2.2	4264.3 (1299.8)	Hyaloclastite	Incipient	None observed	Brown, isopachous smectite 1. Scattered dissolution of shards.
R0516 9.3	4291.4 (1308.0)	Hyaloclastite	Incipient	Numerous tubules penetrate grain margins. Many appear braided.	Brown, isopachous smectite 1 with RSGR. Some dissolution of glass.
R0525 8.33 to 8.45	4329.35 (1319.6)	Hyaloclastite	Incipient	Sparse tubules along grain margins and adjacent to dissolved areas	Brown, isopachous smectite 1. Moderate dissolution common, some grains largely dissolved, but most not affected.
R0548 7.9	4605.5 (1403.8)	Hyaloclastite, polymict.	Smectitic	Tubules common to abundant.	RSGR at grain margins adjacent to tubules. Dissolution adjacent to tubules. Three smectites Brown pore-lining smectite 1, an earlier pore-lining smectite, and green pore-lining smectite 2. Pore-filling and grain-replacing green smectite. Phillipsite pore-fillings.
R0575 5.7	4850.8 (1478.5)	Hyaloclastite	Smectitic	Abundant, extend from grain margin or margin of RSGR areas	Dissolution, RSGR, green grain-replacing smectite; pore-lining and pore-filling smectites, phillipsite.
R0618 1.8	5140.4 (1566.8)	Hyaloclastite, polymict	Smectitic		Smectite replaces Ol and sideromelane, some palagonite; brown and green pore-lining smectites 1 & 2, pore-filling smectite, phillipsite.
R0620 3.75	5162.85 (1573.6)	Hyaloclastite, polymict	Palagonite over-printing smectitic	Tubules present, some focus on Ol	Smectite replacing Ol, RSGR, palagonite; brown and green pore-lining smectites 1 & 2, pore-filling smectite, phillipsite.
R0624 2.8–3.0	5202 (1585.6)	Basalt conglomerate	Little or no sideromelane		Ol to smectite and zeolite, some corrosion of grains and replacement by smectite 1; brown and green pore-lining smectites, 1 & 2, phillipsite, chabazite.
R0675 3.0	5701.1 (1737.7)	Hyaloclastite	Palagonitic	Tubules not common	RSGR rare, palagonite, brown and green pore-lining smectite 1 & 2, Ca-silicate, chabazite.

Table 1. (continued)

Run and dist. below run top, ft	Subsea depth, ft (m)	Lithology	Alteration	Tubules	Alteration features
R0710 2.1–2.5	6084.9 (1854.7)	Hyaloclastite	Palagonitic	Tubules associated with RSGR	Dissolution, some Ol to smectite, RSGR, palagonite; brown and green pore-lining smectite 1 & 2, phillipsite, chabazite.
R0714 6.6–6.7	6173.2 (1881.6)	Hyaloclastite	Palagonitic overprinted on contact metamorphic	Tubules rare, associated with RSGR	Dissolution, RSGR., Ol to smectite in basalt frags. Palagonite (shows zones), brown and green pore-lining smectite 1& 2, phillipsite, Ca-silicate, chabazite, analcime.
R0715 14.1–14.2	6199.7 (1889.7)	Hyaloclastite	Palagonitic overprinted on contact metamorphic	None observed	Dissolution with replacement by zeolite and clay, palagonite; geopetal pore-fillings common, brown and green pore-lining smectite 1 & 2, phillipsite, Ca-silicates, chabazite, analcime, possibly gypsum.
R0718 6.0–6.5	6247.6 (1904.3)	Hyaloclastite	Palagonitic	None observed	Palagonite; brown and green pore-filling smectite 1 & 2, phillipsite, chabazite.
R0733 10.5–10.9	6504.5 (1982.6)	Hyaloclastite, bedded	Palagonitic	Tubules from RSGR into palagonite	Dissolution of grains, RSGR, palagonite, brown pore-lining smectite 1, phillipsite, Ca-silicate, chabazite.
R0740 14.2–14.3	6577.3 (2004.7)	Pillow margin and hyaloclastite	Palagonitic	Tubules abundant, from RSGR into palagonite & sideromelane	Ol to smectite, dissolution (w. brown clay coatings on residual nodules), RSGR, palagonite; brown pore-lining smectite 1, phillipsite, chabazite.
R0771 10.5–10.9	7130.3 (2173.3)	Hyaloclastite	Palagonitic	None observed in palagonite or sideromelane, may be some in plagioclase	Palagonite; brown and green pore-lining smectites 1 & 2, phillipsite, Ca-silicates, chabazite.
R0774 3.5–3.6	7190.25 (2191.6)	Hyaloclastite	Palagonitic	Tubules rare, Spectacular fibers extending from plagioclase may be devitrification features	RSGR, palagonite; brown and green pore-lining smectites 1& 2, phillipsite, Ca-silicate, chabazite.
R0777 0.0–0.6	7251.1 (2210.1)	Polymict lapilli tuff	Palagonitic	None observed	Palagonite, zoned; brown and green pore-lining smectites 1 & 2, phillipsite, chabazite.
R0844 21.8–21.9	8267.9 (2520.1)	Hyaloclastite	Palagonitic	None observed	Palagonite; brown and green pore-lining smectites 1& 2, phillipsite, Ca-silicate, chabazite.
R0852 12.35–12.65	8417.6 (2565.7)	Hyaloclastite	Palagonitic	Rare tubules, extend from RSGR-like material into palagonite	RSGR, palagonite; brown and green pore-lining smectites 1 & 2, phillipsite, Ca-silicate, chabazite.
R0866 5.5–5.6	8848.1 (2696.9)	Hyaloclastite	Palagonitic	None observed	Palagonite; brown and green pore-lining smectites 1 & 2, geopetal fillings, phillipsite, Ca-silicates, chabazite.
R0894 7.3–7.5	9011.4 (2746.7)	Hyaloclastite	Palagonitic	None observed	Palagonite; brown and green pore-lining smectites 1 & 2, phillipsite, Ca-silicates, chabazite.
R0911 18.3–18.45	9241.4 (2816.8)	Hyaloclastite	Palagonitic	None observed	Palagonite; brown and green pore-lining smectites 1 & 2, geopetal partial pore-fillings, phillipsite, Ca-silicates, chabazite.

Table 1. (continued)

Run and dist. below run top, ft	Subsea depth, ft (m)	Lithology	Alteration	Tubules	Alteration features
R0918 18.65–18.95	9365.7 (2854.7)	Hyaloclastite	Palagonitic	None observed	Palagonite; brown and green pore-lining smectites 1 & 2, phillipsite, Ca-silicates, chabazite.
R0923 14.9–15.3	9430 (2874.3)	Hyaloclastite	Palagonitic	None observed	Palagonite; brown and green pore-lining smectites 1 & 2, phillipsite, Ca-silicates, chabazite.
R0930 1.5–1.8	9561.6 (2914.4)	Hyaloclastite	Palagonitic	None observed	Palagonite; brown and green pore-lining smectites 1 & 2, phillipsite, Ca-silicates, chabazite.
R0930 6.5	9567.4 (2916.2)	Hyaloclastite	Palagonitic	None observed	Palagonite; brown and green pore-lining smectites 1 & 2, phillipsite, Ca-silicates, chabazite.

a RSGR, reddened smectitic grain replacement.

loclastite are fresh, although smectite has replaced some in part or entirely.
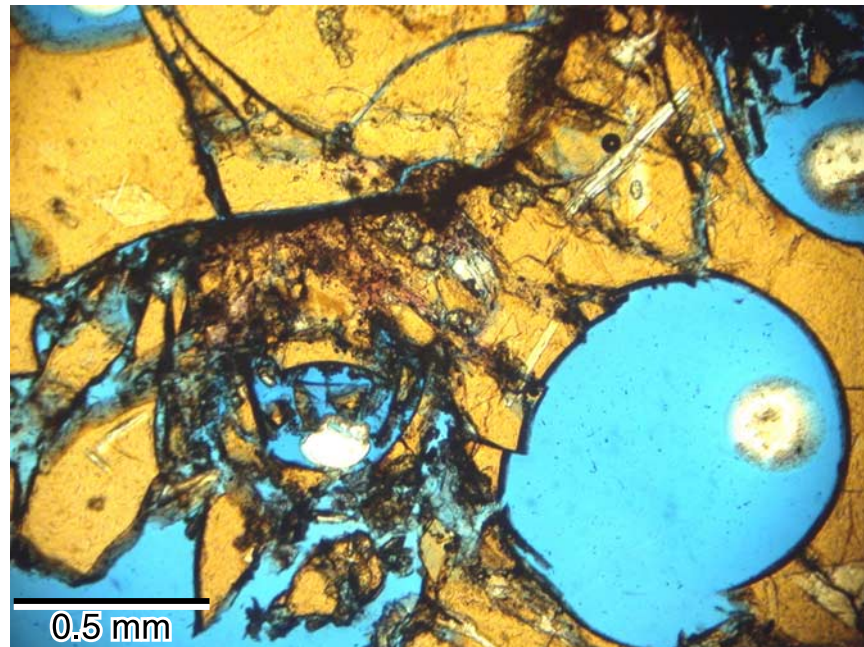
3.2. Fracturing

[12] Except for samples that are contact metamorphosed, virtually all hyaloclastite samples display evidence of fracturing of grains (Figures 2 and 3). Frequently, fractures originate at points of contact between grains and radiate outward along gently curving trajectories. None of the fractures crosses the sample as a whole, so they represent the breakage of individual grains too weak to support the weight of overlying material. Many samples contain accumulations of small fragments in spaces between grains. Particles in some accumulations appear to be fragments of the walls of vesicles. These accumulations are interpreted as the result of crushing of sideromelane grains. They are now cemented in place with smectite and zeolite into the lower side of the pores and are interpreted as geopetal structures. In all samples where both smectite and fractures are present, including those with geopetal accumulations, fractures are coated with the earliest form of smectite (brown, pore-lining smectite 1).

3.3. Smectite

[13] Smectite is a very common alteration phase in HSDP hyaloclastites, making up 4 to 32% of the whole rock. It occurs in four major forms that are petrographically distinct (Figures 2 and 4). The forms of smectite developed in specific order in the alteration history in each sample. Brown pore-lining smectite 1 was the first smectite to form, followed by reddened grain-replacing smectite, pale green pore-lining or pore-filling smectite 2 and pale-green grain-replacing smectite (see below). While unequivocal petrographic distinction among these forms of smectite is routine, chemical compositions of the forms overlap (Table 2, Figure 5).

3.3.1. Brown, Pore-Lining Smectite 1

[14] Smectite forms pore-lining, isopachous to spherulitic rims on grains, including extending back into fractures, where they exist (Figures 2, 3, and 6). Optical character and cursory X-ray diffraction

Figure 3. Fractured hyaloclastite shards in a sample from 1106.7 mbsl, in the zone of incipient alteration. Aside from the obvious fracturing, the lack of any alteration of the glass itself and the lack of well-developed smectite coatings is indicative of this zone. Sample is impregnated with blue-dyed epoxy and imaged in plane polarized light.

indicate this material is a smectite. Electron microprobe analyses indicate it is a saponite (Table 2, Figure 5). This material appears brown in plane-polarized transmitted light, especially compared to other, later smectites in the same samples. Flakes in brown pore-lining smectite 1 are so arranged that the material has an aggregate birefringence with the fast ray perpendicular to the surface of the grain (Figure 4a). In a given sample, the thickness of the smectite 1 rims is approximately the same, except where spherulites have developed. Rims are commonly 5 to 10 μm thick, but in a few samples are up to 20 μm and are vanishingly thin in some. Spherulites have developed at points in the pore lining smectite. Commonly, they are about 10 to 20 μm in diameter, and comprise clay with an aggregate birefringence with the fast ray radial to the spherulite.

[15] In each sample, smectite 1 coats grains of all types, including sideromelane shards, basalt fragments, and crystals of olivine (Figure 2). Coatings are not present at points of contact between grains. The outline of the shard beneath the smectite is angular, but the outline of the smectite layer has rounded corners. These observations imply that the

smectite is a passive grain coating, rather than a marginal replacement of sideromelane. Isopachous rims are characteristic of formation in water-filled voids, as opposed to the funicular distribution characteristic of formation in pores with water in the smaller spaces but bubbles of air or some other immiscible fluid in the centers of larger pores [c.f. *Thorseth et al.*, 1992, their Figure 1c].

3.3.2. Green, Pore-Lining or Pore-Filling Smectite 2

[16] A second form of pore-lining and pore-filling smectite overlies the brown pore-lining smectite 1 (Figures 2, 4a, and 6). Smectite 2 has distinctive optical characteristics; it is pale green in plane-polarized light and has somewhat higher aggregate interference colors than smectite 1, although still in the first order. Finally, pore linings of smectite 2 have aggregate interference with the fast ray parallel to the underlying surface, not perpendicular to it as in the brownish smectite 1 (Figure 4a).

[17] Smectite 2 occurs in isopachous pore linings about 3 to 5 μm thick. Where both smectites 2 and 1 are present, smectite 2 occurs on the side concentrically inward to the pore in those samples. Several

samples exist, all from shallower than 1335 mbsl, which contain smectite 1 but no smectite 2. Few samples contain smectite 2 and no smectite 1. In only one sample, from 1403.6 mbsl, a greenish pore-lining smectite, in a layer a few micrometers thick with the same aggregate optical orientation as smectite 2, occurs beneath smectite 1, immediately adjacent to the surface of the hyaloclastite shard (Figure 4a).

[18] Smectite of very similar appearance to green, pore-lining smectite 2 fills pores in three samples between 1403.6 and 1573 mbsl, defining a distinctive zone of alteration of the hyaloclastites (see below). This smectite has the same apparent color as the pore-lining variety, but does not have a consistent optical orientation (Figure 4c).

3.3.3. Reddened Smectitic Grain Replacement

[19] This is a complex of minerals - dominantly composed of smectite - intergrown on the micrometer scale (Figures 4a, 4b, and 7a). Masses or patches of this complex of minerals extend inward from margins of sideromelane fragments as though they radiated from a single point or grew from the whole margin. They may have nucleated from external grain surfaces, vesicle margins, or from the walls of fractures that cut across the grains. The masses are irregularly distributed along the margins from which they project, rather than forming a replaced layer of uniform thickness. The masses
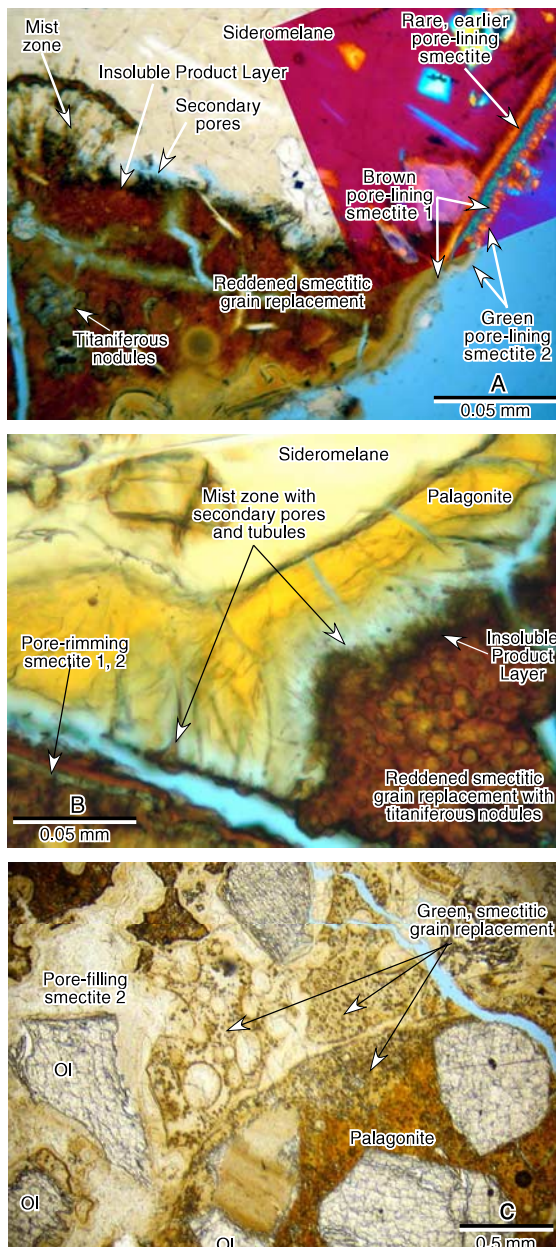
Figure 4. (opposite) Smectite in HSDP hyaloclastites. (a) Photomicrograph showing features of reddened smectitic grain replacement in a sample from the zone of smectitic alteration, 1403.8 mbsl. Blue areas in mist zone show small secondary pores where glass dissolved. Sample is impregnated with blue-dyed epoxy. Most of photograph is shown in plane polarized light. Inset area on right, imaged with crossed polarizers and 1st order red plate inserted, shows three layers of pore-lining smectite with differing optical orientation. The innermost of these layers is present only in this sample. (b) (Compare with Figure 4a.) Reddened smectitic grain replacement with titaniferous nodules, insoluble product layer , and mist zone in a sample from the zone of normal alteration, indicated by the presence of palagonite. The tubules from the mist zone cross a porous zone (bluish from dyed epoxy); the reddish lining of the tubules preserves their integrity through this area. 1881.6 mbsl. (c) Smectite filling of pores and green smectitic grain replacement filling dissolved shards or replacing shards from the zone of smectitic alteration. Outlines of vesicular shards are preserved with brown smectite coatings, and interior of shards show titaniferous nodules suspended in smectite filling of pore. Primary pores are also lined with isopachous to spherulitic pore lining smectite 1 and 2 and filled with green pore-filling smectite 2. Olivine grains (Ol) are partially dissolved and replaced by smectite, again a variety that also resembles smectite 2. Outer margin of shard in lower right is converted to smectite, inner part to gel palagonite. Sample is impregnated with blue-dyed epoxy and imaged in plane polarized light, 1566.7 mbsl.

Table 2. Electron Microprobe Analyses of Smectite From the HSDP2 Phase 1 Drill Core

Meters bsl	1238	1426	2817	2211	2747	2817	1586	1426	1855	2530
Type[a]	1	1	1	2	2	2	O	R	R	R
Na_2O	0.38	0.42	0.13	0.38	0.34	0.30	0.23	1.20	0.37	0.29
MgO	13.57	12.62	12.72	12.50	15.03	16.87	22.80	9.76	13.23	17.87
Al_2O_3	10.30	14.56	9.74	7.76	10.49	7.80	7.81	14.04	10.28	10.82
SiO_2	49.91	49.26	44.16	47.06	47.17	43.62	50.51	48.01	46.21	41.26
P_2O_5	n.a.	n.a.	n.a.	n.a.	n.a.	n.a.	n.a.	0.08	0.08	0.00
K_2O	0.71	0.43	0.30	0.29	0.17	0.08	0.31	0.58	0.21	0.19
CaO	1.27	3.03	3.64	2.19	2.92	1.55	1.08	3.08	4.80	4.77
TiO_2	0.53	0.04	0.73	0.28	0.47	0.34	0.18	0.40	0.19	3.40
MnO	0.14	0.14	0.26	0.47	0.05	0.31	0.00	0.16	0.22	0.14
FeO	9.07	8.74	14.12	18.70	12.42	9.59	7.97	12.83	11.69	11.08
Total	85.88	89.24	85.80	89.63	89.06	80.46	90.89	90.14	87.28	89.82
Cations on the Basis of 22 Oxygen Equivalents										
Si	7.37	7.01	6.85	7.10	6.91	7.00	7.06	6.96	6.94	6.13
Al IV	0.63	0.99	1.15	0.90	1.09	1.00	0.94	1.04	1.06	1.87
sum IV	8.00	8.00	8.00	8.00	8.00	8.00	8.00	8.00	8.00	8.00
Al VI	1.16	1.45	0.63	0.48	0.72	0.48	0.35	1.36	0.76	0.02
Ti	0.06	0.00	0.09	0.03	0.05	0.04	0.02	0.04	0.02	0.38
Mn	0.02	0.02	0.03	0.06	0.01	0.04	0.00	0.02	0.03	0.02
Fe	1.12	1.04	1.83	2.36	1.52	1.29	0.93	1.55	1.47	1.38
Mg	2.99	2.68	2.94	2.81	3.28	4.04	4.75	2.11	2.97	3.95
sum VI	5.35	5.19	5.52	5.74	5.58	5.89	6.05	5.08	5.25	5.75
Na	0.11	0.12	0.04	0.11	0.10	0.09	0.06	0.34	0.11	0.08
Ca	0.13	0.08	0.06	0.06	0.03	0.27	0.06	0.48	0.77	0.76
K	0.20	0.46	0.61	0.35	0.46	0.02	0.16	0.11	0.04	0.04
sum IL	0.44	0.66	0.71	0.52	0.59	0.38	0.28	0.93	0.92	0.88
Mg/(Mg + Fe)	0.73	0.72	0.62	0.54	0.68	0.76	0.84	0.58	0.67	0.74

[a] 1, Brown, pore-lining smectite 1; 2, green pore-lining smectite 2; O, replacing olivine.

are clearly replacive, because they contain fresh phenocrysts or microlites and lie within margins defined by pore-lining smectites.

[20] The masses are variably stained red-brown, presumably with ferric hydroxide. The inner edge of the masses is generally more intensely more stained than the rest (Figure 4). BSE imaging (e.g., Figure 7a), X-ray dot mapping, energy dispersive qualitative analyses, and wavelength dispersive quantitative analyses have all been used to identify smectite, titaniferous spherules or nodules, and a Ca-phosphate (hereafter referred to as ''apatite'') in these red-stained masses . Petrographically, faint birefringence suggests the presence of smectite, and the titaniferous nodules are clearly visible (e.g., Figure 4b). Chemically, the smectites in these reddened grain-replacing masses are distinguishable from pore-lining smectites by having higher content of Na + K + Ca, but their Mg/(Mg + Fe) and Al/(Al + Si) contents overlap those of other smectites (Table 2, Figure 5). Compositionally, the

titaniferous spherules contain 40–50 wt.% TiO_2, with lesser amounts of CaO, SiO_2, FeO, and Al_2O_3 (Table 3), and therefore mineralogically can not be composed solely of titanite or any pure variety of TiO_2.

3.3.4. Tubules Associated With Reddened Smectitic Replacement

[21] The inner margin of these replacement complexes, adjacent to unaltered sideromelane, is marked by an abundance of small tubules in villiform masses (Figures 4 and 7). Tubules may extend into unaltered glass adjacent to the reddened replacement or into palagonite (and possibly sideromelane beyond). Tubules, their walls marked by reddish material, may also cross a zone of voids between the reddened replacement and sideromelane or palagonite (Figures 4a and 4b).

[22] In some areas of individual samples from the HSDP core, tubules are present without the asso-
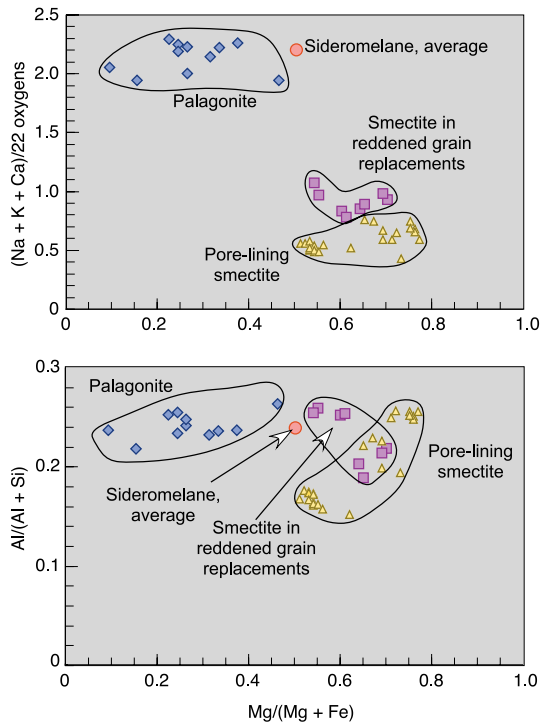
Figure 5. Compositional relationships among pore-lining smectites, palagonitized glass, reddened smectitic grain replacement, and sideromelane. Compositionally, the smectitic grain replacement and pore-lining smectites resemble each other, although the consistently higher non-interlayer cation content of the former suggest that they are less pure (i.e., the replacement smectite contains small amounts of residual primary minerals or other secondary alteration products.) Palagonite differs from the smectites in both composition of Na + Ca + K and in Mg/(Mg + Fe), and has evolved in a different direction from sideromelane.

ciated red-brown smectitic grain replacement, but such replacement is not present without tubules. In some examples, tubules appear to curve toward olivine phenocrysts, but do not visibly extend into the crystal phase. This tubule-rich zone and a zone of darker red staining on the smectitic grain replacement adjacent to it resemble the mist zone and insoluble product layer (IPL) of *Morgenstein and Riley* [1975] [see also *Melson and Thompson*, 1973]. Tubules closely resemble some figured by *Fisk et al.* [1998] as well as the pit-textures described by *Thorseth et al.* [1992] and interpreted by them as being of microbial origin.

[23] To test the microbial origin of tubules, several samples were stained with a DNA sensitive probe,

DAPI (4′, 6-diamidino-2-phenylindole), using procedures developed for staining DNA in bacteria on filters. Characteristic stains, indicating the presence of DNA, developed at the points where tubules in sideromelane reached the surface of thin sections (Figure 8). Samples with no visible tubules did not develop such stains.

[24] All samples containing the complex of reddened smectite, titaniferous spherules, apatite, and villiform masses of tubules also include pore-lining smectite 1. The grain-replacive complex is also present in samples displaying smectite 2, and in many samples that contain palagonite. Hence, this combination of reddened smectitic grain replacement and tubules is a characteristic form of alteration in the HSDP samples. However, tubules and reddened smectitic grain replacement are absent from all samples but one below 2200 m depth and is poorly developed or not present in the youngest hyaloclastites. The complex of reddened smectite, titaniferous spherules, apatite, and tubules form early in the history of the rocks directly from sideromelane, without an intermediate palagonite stage.

3.3.5. Green Smectitic Grain Replacement

[25] In samples from the zone between 1406 and 1573 mbsl, smectitic masses replacing grains and grain margins are pale green in thin section and petrographically resemble pore-filling smectite 2 (Figure 4c). These masses contain titaniferous spherules, like those in the reddened smectitic grain replacements described above, but lack the red color and no tubules have been observed in association with them. Like the reddened masses, green masses project from margins of grains. Green smectitic grain replacement is restricted to samples that display green pore-filling smectite and these two varieties of smectite closely resemble each other petrographically.

3.4. Palagonite

[26] All hyaloclastite samples below 1573 mbsl in the HSDP 2 Phase 1 core display replacement of shards with palagonite (Figures 2, 4b, 6, and 9). Palagonite is a yellow-orange isotropic material that differs from sideromelane in its chemical composition (Figure 5, Table 3). Pala-
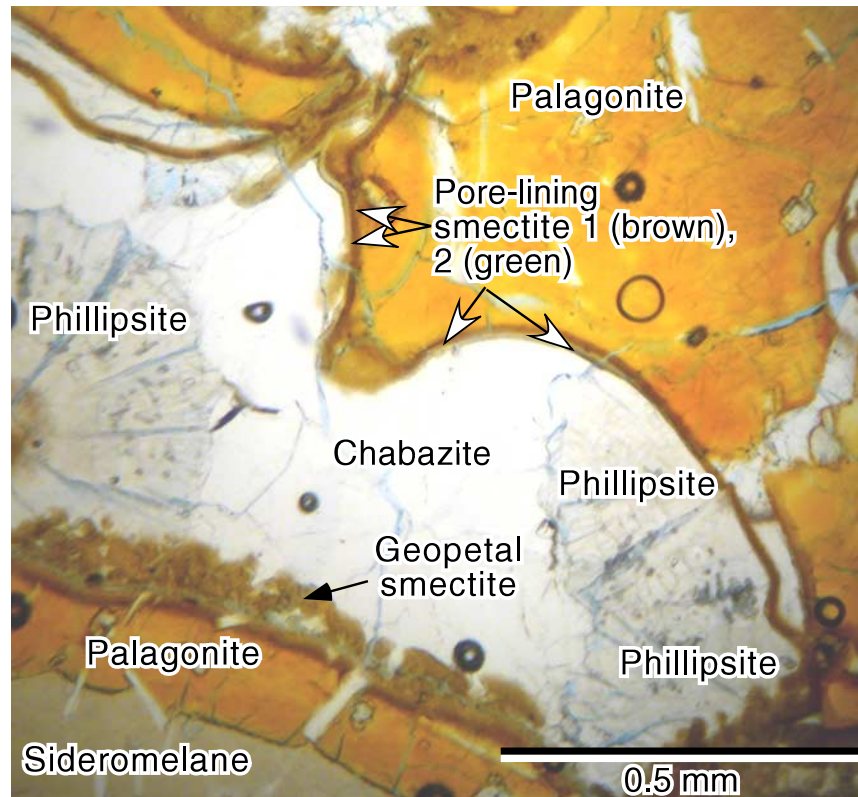
Figure 6. Pore-filling chabazite and radiating masses of bladed phillipsite crystals in the zone of palagonitic alteration. Pores are lined with pore-lining smectites 1 and smectite 2. Phillipsite spherulites nucleate at breaks in the rim of smectite 1. The rim of smectite 2 gradually increases from zero thickness in the inner part of the phillipsite spherulite to normal thickness at its margin, demonstrating simultaneous growth. Remainder of pore is filled with chabazite, except for geopetal accumulations of smectite clots in lower left and upper left. Shards show marginal conversion to palagonite and larger ones have preserved sideromelane. 1889.7 mbsl. Sample has been impregnated with blue-dyed epoxy and was imaged in plane polarized light.

gonite is depleted in all major elements, except it is enriched in TiO_2 and H_2O and total iron as FeO is unchanged, with respect to adjacent sideromelane (Table 3) [*Walton et al.*, 2002]. In the HSDP 2 Phase 1 drill core, palagonite has a remarkably consistent composition, irrespective of depth (P. Schiffman, unpublished data, 2000, 2001). In terms of Mg/(Mg + Fe) and Na + K + Ca/22 oxygens, the change from sideromelane to palagonite represents a trend opposite to that from sideromelane to smectite (Figure 5).

[27] Palagonite completely replaces some small shards and marginally replaces larger ones. Its replacive nature is shown by included vesicles, phenocrysts, and microlites and by its existence within the margins of the shards, as defined by early brown pore-rimming smectite 1. Palagonite develops on the external margins of shards, on fractures,

and on the margins of vesicles. Marginal bands are 0.01 to 0.5 mm thick and appear uniform on grains, except for the variations caused by the angle of cut across the grain. On fractures or vesicles, the replaced margins may not be as wide as on the external margins of the same shard.

[28] In most samples, palagonite is not markedly banded, but displays a uniform appearance across its entire width. In a few samples, it displays some different appearances, chiefly a few concentric layers that differ in having minute markings that resemble pits in them (Figure 9). The inner contact of palagonite with sideromelane is smooth and sharp. Palagonite may engulf tubules in mist zones that extend inward from the margins of the shard or from dark brownish red, nearly opaque IPLs that form the inner boundary of patches of reddened smectitic grain replacements (Figure 4b). Some
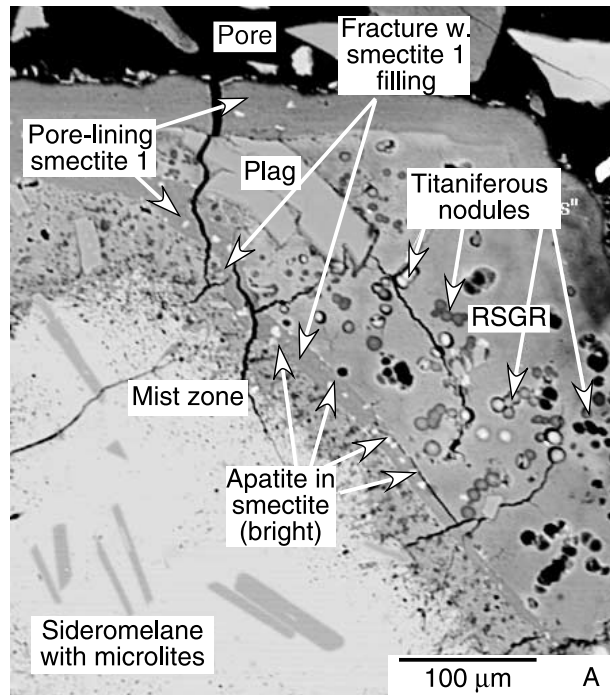
Figure 7. (a) Backscattered-electron image of reddened smectitic grain replacement (RSGR) and pore-lining smectite from 1426 mbsl. Within the zone of smectite alteration, a sideromelane shard has been coated with smectite and partially replaced by reddened smectitic grain replacement. An early fracture running from the upper lower left to the lower right of the BSE micrograph has been filled with smectite containing abundant apatite inclusions. The smectitic grain replacements contains abundant inclusions of spherulitic, titaniferous nodules (<10 um in diameter). A mist zone (containing tubules that appear as black and gray dots) separates the smectitic grain replacement from sideromelane (containing plagioclase microlites). (b) Secondary electron micrograph of vesicle wall and tubules from 1478.5 mbsl. Vesicle contains pore-lining smectite.

tubules extend beyond the gel palagonite zone into unaltered sideromelane.

[29] Conversion of sideromelane to palagonite appears to be an isovolumetric process. The boun-dary of many shards cuts across both sideromelane and crystals, either phenocrysts of olivine or micro-lites of plagioclase. In all shards that have under-gone marginal conversion to palagonite, the outer boundary is smooth, neither forming meniscus-like

Table 3. Electron Microprobe Analyses of Sideromelane, Palagonitized Glass, Titaniferous From the HSDP2 Phase 1 Drill Core

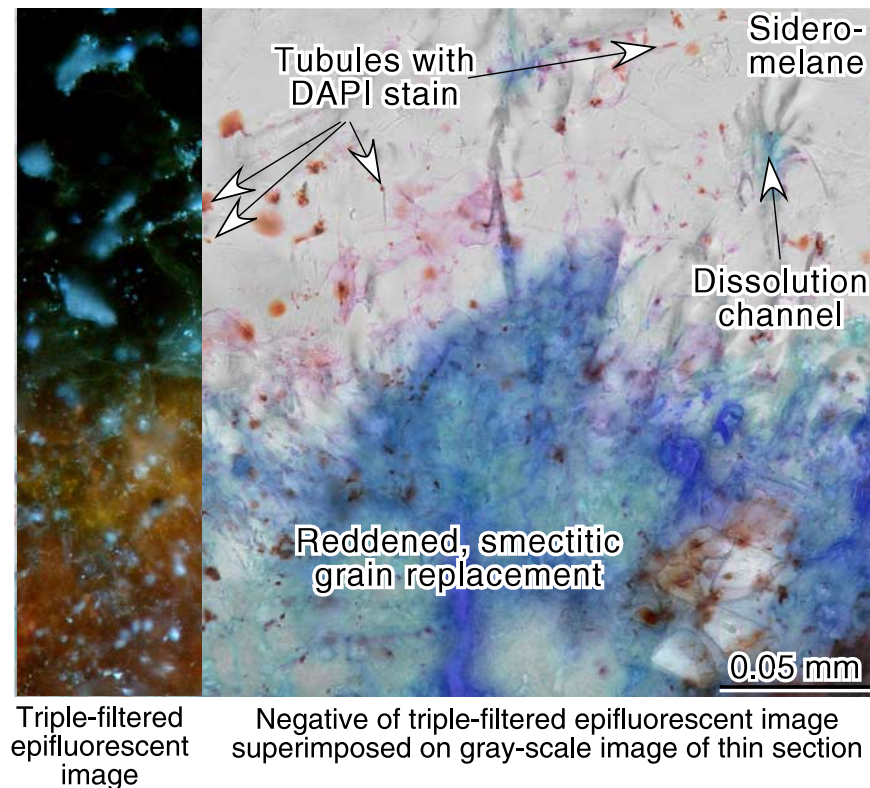| Meters bsl	Sideromelane (average)	Palagonitized Glass				Titaniferous Nodules	
		1855	1883	2211	2915	1426	1426
Na_2O	2.21	0.36	0.90	0.70	0.52	n.a.	n.a.
MgO	6.74	1.88	2.33	1.04	2.00	n.a.	n.a.
Al_2O_3	13.46	11.62	11.29	11.09	12.94	3.3	2.35
SiO_2	50.99	43.65	42.30	44.29	44.06	8.28	7.61
P_2O_5	0.34	0.28	0.44	0.20	0.20	n.a.	n.a.
K_2O	0.38	0.22	0.32	0.34	0.36	n.a.	n.a.
CaO	11.13	12.00	10.84	10.54	11.27	7.57	10.06
TiO_2	2.65	4.27	3.77	4.91	4.34	37.67	48.21
MnO	0.17	0.07	0.05	0.03	0.10	n.a.	n.a.
FeO	10.90	7.70	13.60	7.62	7.51	4.34	3.24
Total	98.97	82.05	85.84	80.76	83.30	61.17	71.47
Cations on the Basis of 22 Oxygen Equivalents							
Na	0.57	0.11	0.26	0.22	0.16		
Mg	1.35	0.45	0.53	0.25	0.46		
Al	2.13	2.19	2.11	2.11	2.39		
Si	6.84	6.98	6.69	7.16	6.92		
P	0.04	0.04	0.06	0.03	0.03		
K	0.07	0.05	0.06	0.07	0.07		
Ca	1.60	2.06	1.85	1.82	1.90		
Ti	0.27	0.51	0.46	0.60	0.51		
Mn	0.02	0.01	0.01	0.00	0.01		
Fe	1.22	1.03	1.84	1.03	0.99		
sum	14.11	13.43	13.87	13.29	13.44		

curves up to a projecting crystal, which would indicate shrinkage, nor forming a dimple over the crystal, which would indicate expansion in forming palagonite (Figure 2). Furthermore, where gel-palagonite formed at vesicle margins, there is no evidence of compression or tension in the gel palagonite, as would be expected if the volume changed. Point contacts between shards are common, and if expansion had occurred, such contacts would be penetrative. Many other investigators [e.g., *Jercinovic et al.*, 1990; *Stroncik and Schmincke*, 2001] have also argued that formation of gel palagonite is isovolumetric based on similar observations.

[30] Thickness of palagonite rinds was measured on ten randomly selected grains in each thin section of samples from the zone of palagonitic alteration (Figure 10). Grains were chosen where the cross hairs landed on the palagonite rim, and the measurement made at that point. Values for each thin section were averaged and plotted. Measured thickness of the rim depends upon the actual thickness and the angle of cut of the thin section with respect to that rim, so estimates from this

source are probably on the high side. This is partially offset by underestimates of rim thickness based upon grains or parts of grains that were completely converted to palagonite so rims from opposite sides had grown to merge. The plot shows variability of rim thickness at any depth range, but no tendency to increase down hole, despite low precision of the measurements.

3.5. Zeolites

[31] Phillipsite occurs in all hyaloclastite samples from 1403 mbsl to the bottom of the core. It makes up <1% to 6% of the samples in which it occurs. Phillipsite was identified from its petrographic appearance, X-ray diffraction studies of separates and thin sections, and electron microanalysis (Table 4, Figures 2, 6, 11, and 12). Phillipsite occurs in either fibroradial masses or spherulites of prismatic crystals in primary pores and fractures in samples from the zones of smectitic and palagonitic alteration (Figures 2 and 11). Fibroradial masses are small, up to about 20μm radius, or they form the core of the larger spherulites of prismatic

Triple-filtered
epifluorescent
image

Negative of triple-filtered epifluorescent image
superimposed on gray-scale image of thin section

Figure 8.   Photomicrograph of sample of reddened, smectitic grain replacement stained with DAPI to detect DNA. The left part shows a DAPI stain on part of the field of view as seen in epifluorescent ultraviolet light with a triple filter. In this configuration, the DAPI stained areas are bluish white. In the rest of the image, which is in optical continuity with the left part, the image in filtered ultraviolet light has been converted to a negative (light blue DAPI stains become red orange), rendered transparent and superimposed on a gray scale view of the same field in plane polarized light. The area of reddened smectitic grain replacement is blue in this view. Numerous examples exist of tubules of the mist zone having DAPI (red orange in right portion of image) stains where they come to the surface of the thin section in the sideromelane. The mist zone here consists of branching dissolution channels as well as smaller tubules. Sample from 1478.5 mbsl.

crystals that are apparently syntaxial overgrowths on favored fibrous crystals. In many spherulites, there is a zone of intergrowth of smectite 2 and phillipsite either at the outside of the fibroradial masses or separating the fibrous and bladed crystals in the spherulites (Figures 6 and 11). Radiating prismatic crystals range to about 0.2 mm long and may display pyramidal terminations.

[32] Chabazite fills primary and secondary pores remaining after formation of smectites, phillipsite, and Ca-silicate. Chabazite was identified by its appearance in thin section, its X-ray diffraction pattern, and its chemical composition (Table 4, Figure 13). Chabazite forms blocky, equant to slightly elongate crystals that are several hundredths to a few tenths of a millimeter long (Figures 2, 6, 9,

and 12). Chabazite occurs only in samples that contain palagonite and vice versa. It is intergrown with margins of Ca-silicate masses, forming very irregular boundaries between the phases.

[33] In the HSDP hyaloclastites, $Al/(Al + Si)$ averages 0.28 for phillipsite and 0.26 for chabazite, with little overlap of the range. Chabazite contains less K than phillipsite, but the range of Ca:Na is similar for the two minerals (Table 4, Figure 13).

3.6. Calcium Silicates

[34] Various hydrous calcium silicates, referred to here as Ca-silicates, form diaphanous-looking masses that partially fill pores, including vesicles, and replace spherulites of early phillipsite (Figures 11, 12, and 14a). Ca-silicate masses range from
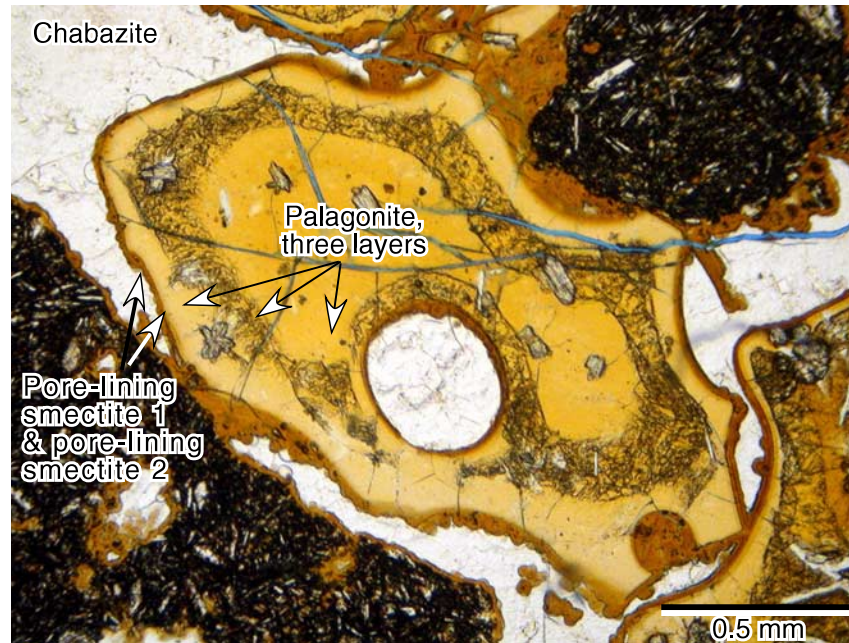
Figure 9. Shard replaced with palagonite. Replacement forms 3 textural layers, inner and outer smooth layers and an intermediate layer with a rough texture. Shards and adjacent basalt fragments are surrounded by isopachous to spherulitic smectite rims and pores are filled with chabazite. 2210.1 mbsl.

pale blue to brown or gray in plane-polarized light, depending upon the degree to which the blue-dyed epoxy has penetrated into them. Generally the cores of the masses are less penetrated than are the rims, so cores appear brown or dark gray in transmitted light, owing to dispersion effects of light passing through them (Figure 10a). They are white in reflected light, probably because they have many voids in them. Electron microanalysis shows these materials contain primarily Ca and Si (Table 5). Because these masses are isotropic, it is unlikely that they are intergrowths of fine-grained calcite with a silica mineral. Hence they are identified as Ca-silicates.

[35] Stoichiometry and anhydrous oxide sums (Table 5) show that one of the Ca-silicates is probably gyrolite ($NaCa_{16}(OH)_8[AlSi_{23}O_{60}] \bullet 14H_2O$). Gyrolite is reported in several other situations where basalt has altered at very low temperatures [e.g., *Honnorez*, 1978, 1981]. Two other Ca-silicates are quite compositionally distinct from the gyrolite. Although both of these are apparently highly hydrous or porous (with oxide sums of 50–55 wt%), one has a Ca/Si ratio close to 0.5 and the other close to 1.3 (Table 5). The compositions of

these phases do not closely match that of any other Ca-silicates found in basalts altered at low temperatures (i.e., truscottite, nekoite, thaumasite, and apophyllite). However, both thaumasite and apophyllite have been conclusively identified in the HSDP 2 Phase 1 core (P. Schiffman, unpublished data, 2001).

[36] In BSE images (Figures 14a and 14b), Ca-silicates exhibit a wide range in gray levels, which appear to reflect their water content. All the Ca-silicates tend to be paragenetically associated with apatite. This association may take the form of intimate intergrowths (e.g., with amygdaloidal gyrolite, Figure 14a) or discrete inclusions (e.g., the bright inclusions within Ca-silicates in Figures 14a and 14b).

3.7. Dissolution

[37] Dissolution of glass in shards is observable in many thin sections. While it is widespread, it is not abundant in any sample. It ranges from minor marginal dissolution to complete dissolution of shards (Figure 15). Where dissolution is complete, the space may be empty, it may contain a residue of
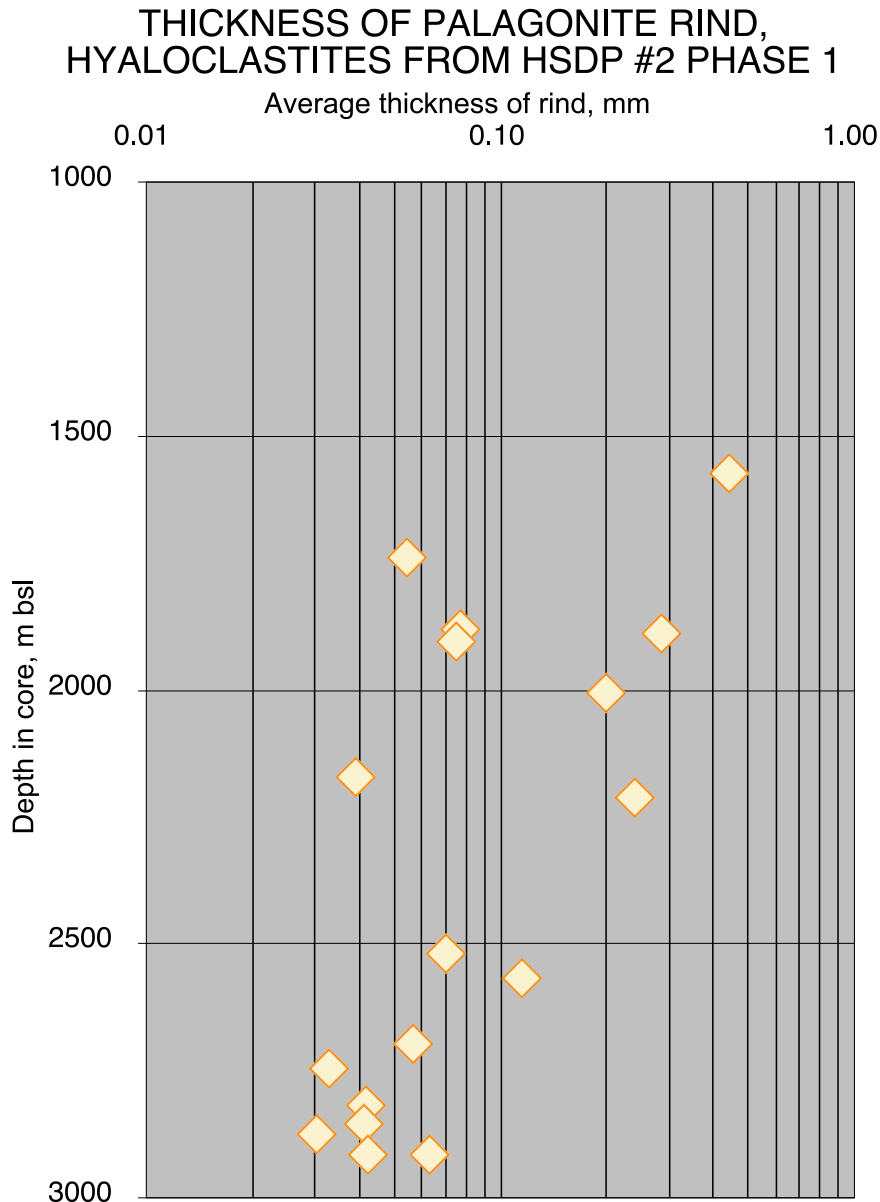
Figure 10.   Average thickness of rinds of palagonite on shards in the zone of palagonitic alteration. Average thickness is widely scattered in each depth range, but shows no increase down hole in the zone of palagonitic alteration.

apparently fresh olivine, plagioclase, and pyroxene microlites, or it may contain scattered titaniferous nodules, similar to those in grain-replacing smectites. Dissolution occurred after formation of pore-lining smectite 1. In samples from the zone of smectitic alteration, dissolved grains may be filled with green, grain-replacing smectite. In samples from the zone of palagonitic alteration, zeolite forms pseudomorphs of the original texture, with the pore-rimming smectite preserving the original outline, microlites revealing their original nature, and tita-

niferous spherules linking them genetically to dissolved shards from the zone of incipient alteration. Dissolution, unlike the replacive processes involved in forming reddened smectitic grain-replacements and palagonite, provides all components of the glass for forming secondary minerals in pores.

3.8. Porosity

[38]   Point counts show that porosity in the zone of palagonitic alteration has fallen to very low levels,

Table 4. Electron Microprobe Analyses of Zeolites From the HSDP 2 Phase 1 Core

|	Chabazite				Phillipsite		
Sample, mbsl	1883	2211	2566	2915	1586	1855	2915
Na_2O	5.11	6.59	4.78	6.73	6.19	5.02	3.21
Al_2O_3	19.57	17.16	19.79	21.62	23.98	19.89	22.78
SiO_2	49.43	53.96	48.22	48.94	49.56	48.71	50.07
K_2O	1.18	1.23	1.44	1.55	5.75	3.83	4.22
CaO	5.20	5.96	6.54	5.50	3.28	3.92	4.61
FeO	0.17	0.01	0.18	0.11	0.00	0.10	0.09
Total	80.66	84.91	80.95	84.45	88.76	81.47	84.98
	24 Oxygens				32 Oxygens		
Sample, mbsl	1883	2211	2566	2915	1586	1855	2915
Si	8.18	8.50	8.02	7.83	10.25	10.81	10.59
Al	3.82	3.19	3.88	4.07	5.84	5.20	5.68
Fe	0.02	0.00	0.02	0.02	0.00	0.02	0.02
Na	1.64	2.01	1.55	2.09	2.48	2.16	1.32
K	0.25	0.25	0.31	0.32	1.52	1.08	1.14
Ca	0.92	1.01	1.16	0.95	0.73	0.93	1.05
sum	14.83	14.96	14.94	15.28	20.82	20.20	19.80

<4% (Figure 16). Porosity when the sediment was deposited was probably much higher. First, granular sediments are deposited with porosity of about 40 to 50% [Pryor, 1973]. Second, an estimate of the initial value of porosity and that at the onset of palagonitization can be developed by measurement of minus cement porosity. Minus cement porosity includes open pores plus primary and fracture pores subsequently filled by cement. It does not include dissolved or replaced grains. The plot of minus cement porosity against depth includes both samples that have undergone palagonitization plus a small number that underwent contact metamorphism (Figure 16). Samples that experienced contact metamorphism and later palagonitization have minus cement porosity averaging 43%. Those that experienced only palagonitization have minus cement porosity averaging 25%.

[39] Contact metamorphic effects will be presented in a future contribution. However, it can be pointed out here that contact metamorphism was an early event and resulted in the crystallization of minerals that enabled the hyaloclastites to resist compaction. Hyaloclastites in contact aureoles also contain a large fraction of highly vesicular shards and noticeably few fractured fragments, unlike most hyalo-

clastites from the zone of palagonitic alteration. Hence the 43% average value is an estimate of the primary porosity of HSDP hyaloclastites. The lower values of minus cement porosity in palagonitized hyaloclastites indicate that all hyaloclastites underwent compaction by crushing before alteration and during the episode of fracturing, except those that experienced contact metamorphism. Subsequent to fracturing, porosity in the hyaloclastites was in the range of 20 to 30%. Much of the decline to the current values reflects precipitation of cements (smectite, Ca-silicates, zeolites) in primary intergranular pores, vesicles, and fractures. Figure 16 shows no decline of porosity with depth over the lower 1.5 km of the boring. Hence, the decline from 20% to 30% porosity to modern values of less than 4% in samples containing palagonite occurred above a depth of 1575 m.

4. Alteration Zones and Sequence

[40] It is convenient to recognize three zones of alteration in samples from the core (Figure 1). Incipient alteration is present in samples from the top of the submarine portion of the core (at 1080 mbsl) to a depth of 1335 mbsl. Smectitic alteration has developed in a thin zone near the top of the
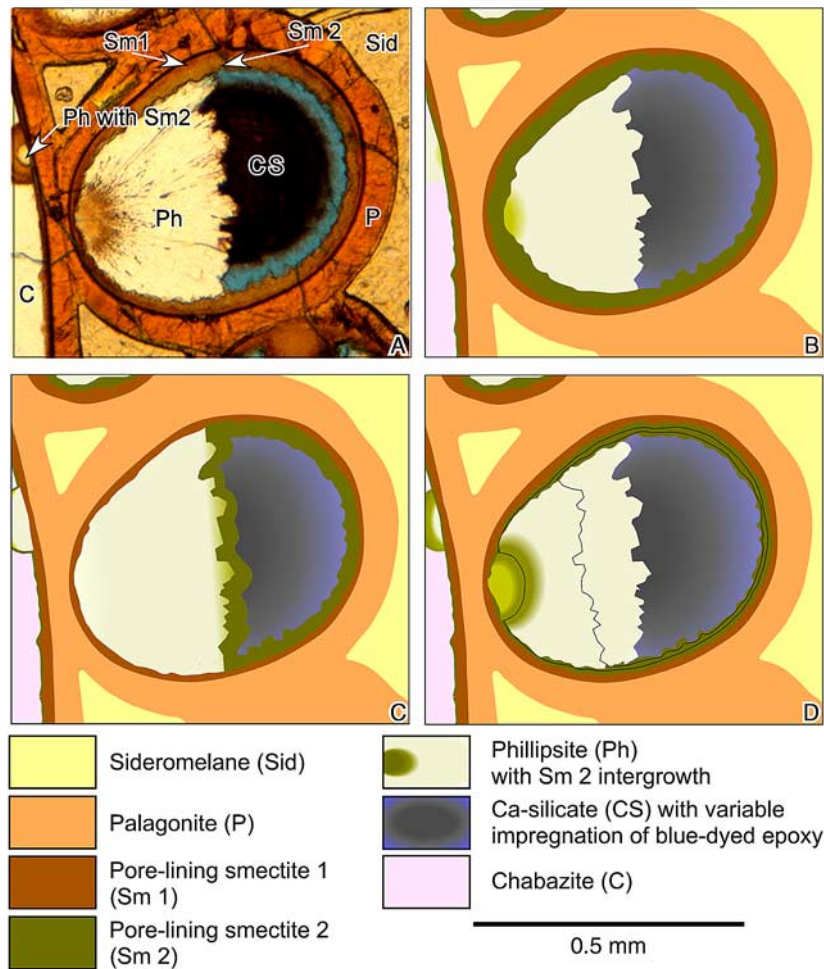
Figure 11. Relative order of formation of pore-lining smectite 2, phillipsite, and Ca-silicate. (a) Photomicrograph showing a vesicle with all three phases forming the filling. A small spherulite of phillipsite projects into the primary intergranular pore on the left. (b, c, d) Sketches of same field of view. (b) Configuration of pore-lining smectite 2 if it formed before phillipsite. (c) Configuration if smectite 2 formed after phillipsite. (d) Configuration if pore-lining smectite 2 and phillipsite grew simultaneously (cf. with Figure 11a).

submarine portion; it is present in samples from 1403 mbsl to those at 1573 mbsl. Palagonitic alteration characterizes all hyaloclastite samples from a depth of 1573 mbsl to the bottom of the core.

[41] Palagonitic and smectitic alteration are later stages of progressive alteration than incipient alteration. Virtually all samples from the zones of smectitic and palagonitic alteration contain essentially the same alteration features displayed in the zone of incipient alteration as well as their own characteristic alteration features. However, only one sample containing palagonitic alteration features, the shallowest such sample, from 1573 mbsl,

also displays smectitic alteration features. Furthermore, the characteristic textures and minerals of smectitic alteration cannot easily convert to those of normal alteration. Consequently, smectitic alteration and palagonitization are alternative end products of the alteration as present in the core so far. Palagonitic alteration may overprint smectitic alteration, but smectitic alteration will not convert into palagonitic alteration.

4.1. Sequence of Events

[42] For the most part, textural relationships define sequence of events clearly. For example, formation of brown pore-lining smectite 1 occurred after
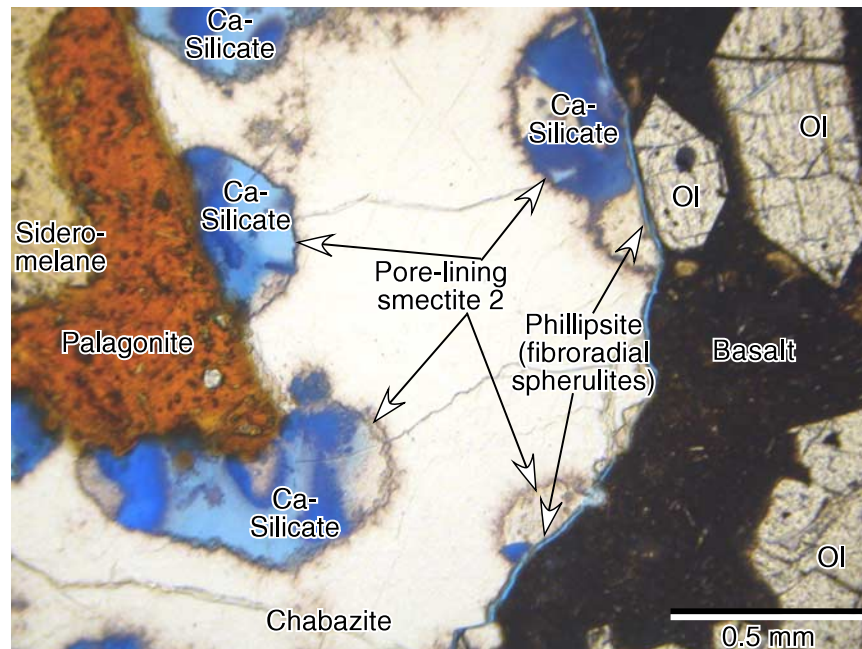
Figure 12. Photomicrograph of pore-filling chabazite with phillipsite spherulites and Ca-silicate pseudomorphs of other phillipsite spherulites, 2915.9 mbsl. Shades of blue indicate degree of imbibition of blue-dyed epoxy into Ca-silicates. Inclusions at margins of chabazite are green pore-lining smectite 2. Basalt fragment on right has pristine olivine phenocrysts (Ol). Hyaloclastite shard on left has marginal conversion to palagonite, but contains unaltered sideromelane in interior. Sample is impregnated with blue-dyed epoxy and imaged in plane polarized light.

fracturing, but before dissolution of shards and formation of reddened smectitic grain replacements (with the tubules or mist zone, and insoluble product layer). Abundance and thickness of patches of red-brown grain replacement increase through the interval of incipient alteration, suggesting progressive development. Brown pore-lining smectite 1 coats all fractures and records the shape of the grains before those later processes took place. This form of smectite is not intergrown with any other phases except apatite (Figure 7a).

[43] Other formation sequences require a little explanation. Phillipsite formed by itself, with green pore-lining smectite 2, with Ca-silicates, and finally again by itself (Figure 11). The earlier spherules of fibrous phillipsite crystals nucleated directly on surfaces of hyaloclastite fragments or on brown pore-lining smectite 1. After a period of growth, the spherules were either engulfed in green pore-lining smectite 2 and ceased growing, were engulfed in smectite, but continued to grow into the radiating prismatic form (Figures 6 and 11), or they dissolved (Figure 12). At this point, the Ca-

silicates formed, filling pseudomorphs of phillipsite or vesicles, fractures, or pores in the rock. The radiating prismatic form of phillipsite appears to truncate zonation of Ca-silicates, suggesting that
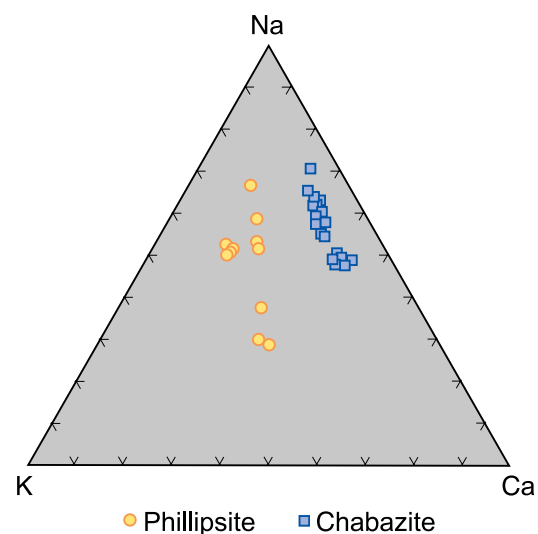
Figure 13. Ternary Na-Ca-K diagram of zeolites from the HSDP-2 Phase 1 drill core. Phillipsite is markedly enriched in K with respect to chabazite.
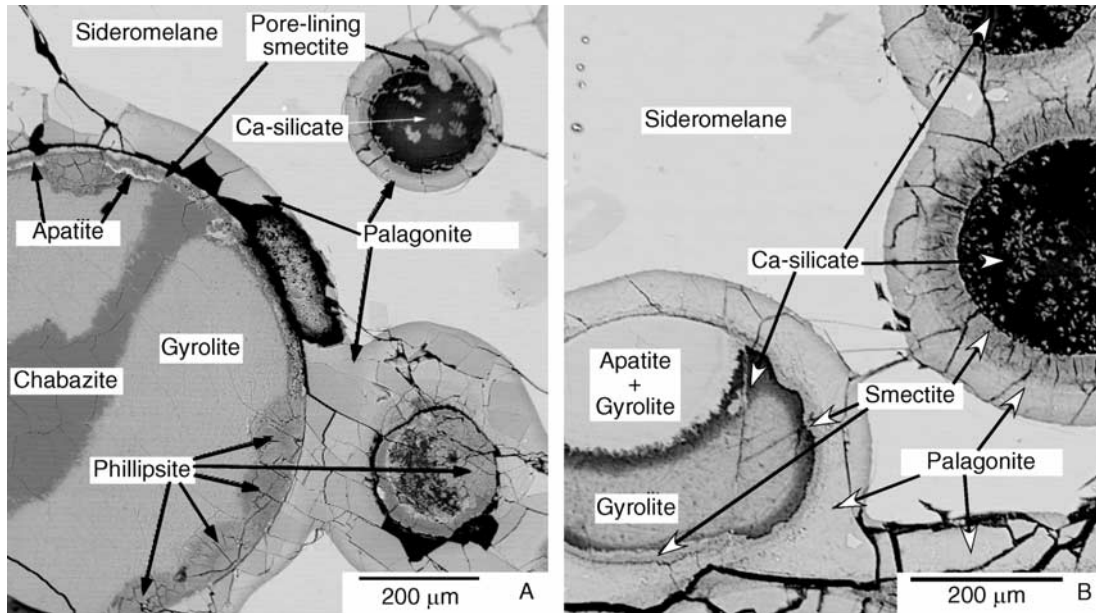
Figure 14. Backscattered-electron images of thin sections. (a) (2747 mbsl) Within the zone of palagonitic alteration, isopachous smectite, with a partial rim of apatite, lines the inner walls of amygdules and gel palagonite replaces sideromelane. The large vesicle on the lower left is filled with spheroidal phillipsite and more massive gyrolite and chabazite. The small vesicle in the upper right is in-filled with an unknown Ca-silicate. (b) (2817 mbsl) Amygdules filled with Ca-silicates. The palagonite- and smectite-lined vesicle on the lower left has been filled with gyrolite, a darker, unknown Ca-silicate, and a brighter mixture of gyrolite and apatite. Vesicles on the upper right are filled with an unknown Ca-silicate.

Table 5. Electron Microprobe Analyses of Calcium Silicates From the HSDP 2 Phase 1 Drill Core

|	Gyrolite		Unknown Ca-silicates		
Sample (mbsl)	2747	2817	2747	2747	2817
Na_2O	0.50	0.42	0.74	0.26	0.82
MgO	0.07	0.01	0.08	0.08	0.07
Al_2O_3	4.81	5.20	3.58	2.66	3.73
SiO_2	49.54	49.99	32.96	22.85	31.42
P_2O_5	0.49	0.37	0.28	0.45	0.25
K_2O	0.10	0.14	0.10	0.07	0.19
CaO	32.80	29.36	15.52	28.42	13.02
TiO_2	0.02	0.01	0.04	0.02	0.03
MnO	0.00	0.00	0.00	0.00	0.00
FeO	0.29	0.20	0.27	0.24	0.04
Total	88.62	85.70	53.57	55.05	49.57
	16 oxygens				
Si	5.48	5.63			
Al	0.63	0.69			
Mg	0.01	0.00			
P	0.04	0.04			
Ti	0.00	0.00			
Mn	0.00	0.00			
Fe	0.04	0.03			
Na	0.11	0.09			
K	0.02	0.03			
Ca	3.88	3.54			
sum	10.21	10.05			
Ca/Si	0.71	0.63	0.50	1.33	0.44
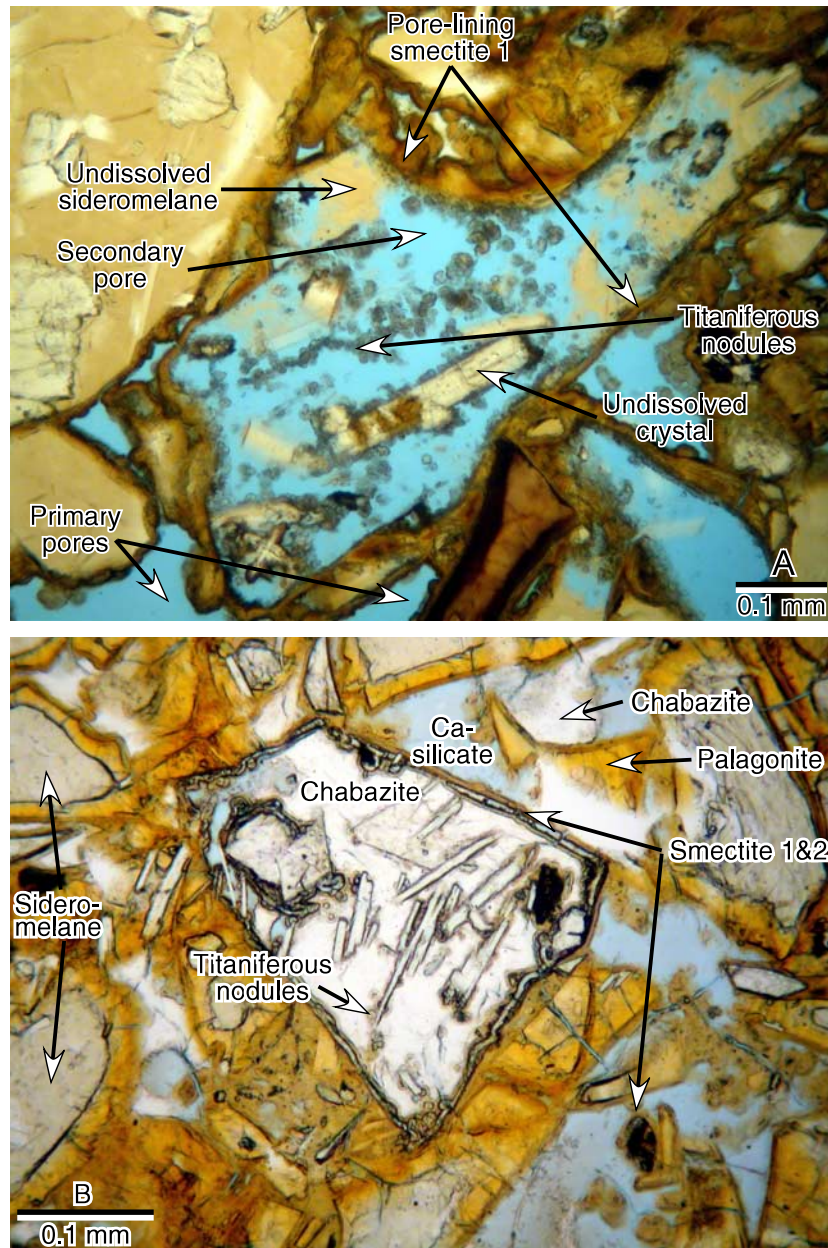
Figure 15. (a) Dissolved shards forming secondary pores in the zone of incipient alteration, 1334.8 mbsl. Shard outlined by pore-lining smectite 1. Titaniferous nodules, phenocrysts, and shreds of glass remain within outline of shard. (b) Dissolved shard in zone of palagonitic alteration, 1982.6 mbsl. Secondary pore is filled by chabazite, but titaniferous nodules and inherited crystals are present. Adjacent shards show palagonite rims. Primary pores are rimmed with pore-lining smectite and filled with chabazite and Ca-silicates (pale blue). Samples are impregnated with blue-dyed epoxy and imaged in plane polarized light.

phillipsite continued to grow after Ca-silicate ceased (Figure 11). Some phillipsite crystals have diffuse terminations in Ca-silicate, suggesting it grew into the voids in the Ca-silicate. While the timing of Ca-silicate formation and growth of green pore-lining smectite 2 can be nicely related

to growth of phillipsite, the timing of green pore-filling smectite and grain replacing smectite cannot be precisely placed.

[44] All samples that contain chabazite also contain palagonite and vice versa. Chabazite fills pores
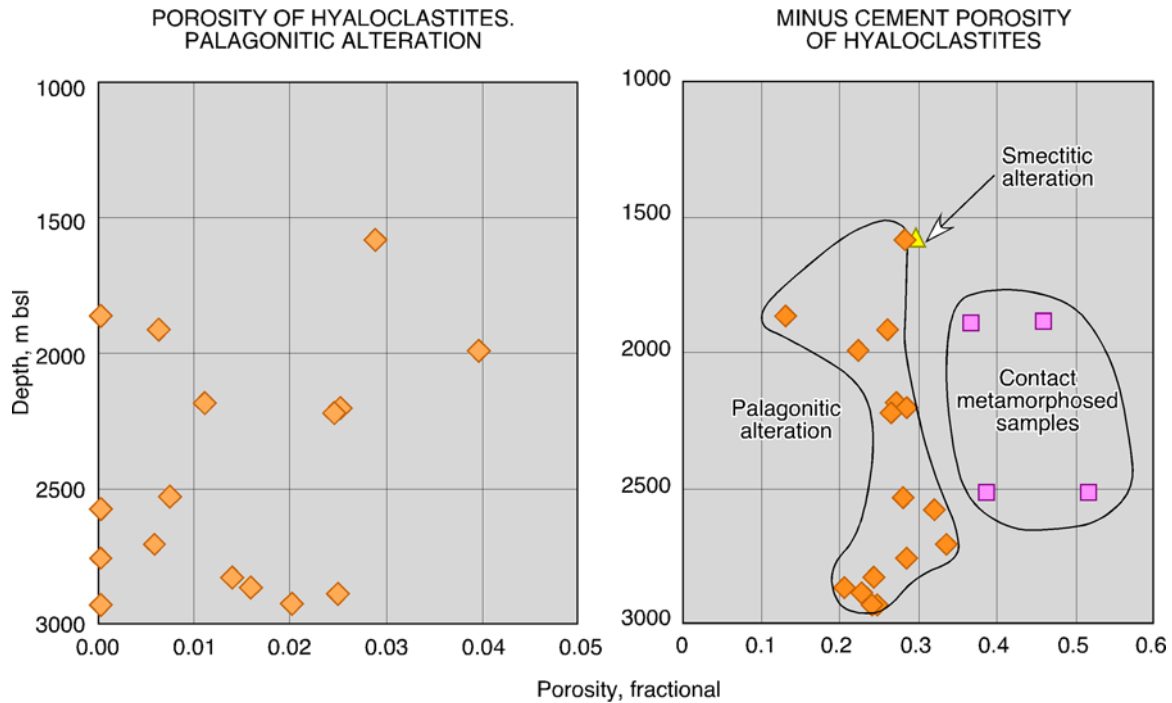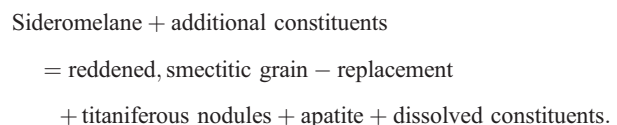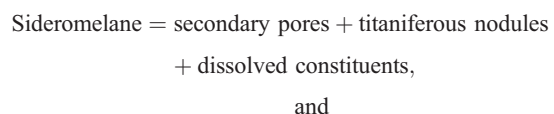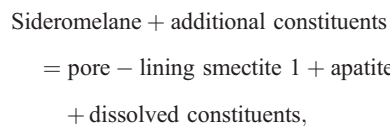
Figure 16. (left) Porosity of samples from the zone of palagonitic alteration in the HSDP 2 Phase 1 core, from point counts. Porosity of samples from this zone is small and varies little down hole. (right) Minus-cement porosity (i.e., remaining primary porosity plus cement in primary pore spaces) of hyaloclastites displaying normal alteration, smectitic alteration, and contact metamorphic features. High minus-cement porosity of contact metamorphosed samples implies both early contact effects (before substantial compaction) and primary porosity values averaging 43%. Precision of individual measurements is low owing to the coarse grain size and consequent small number of points counted on each thin section.

remaining after formation of pore-lining smectite, phillipsite and Ca-silicate, suggesting chabazite is formed late (Figures 1, 6, and 12). All of the other alteration products are present in samples that do not contain chabazite and palagonite, or are convincingly dated as before the formation of palagonite and chabazite. Hence, chabazite and palagonite formation are simultaneous and last in the observed succession.

4.2. Incipient Alteration of Hyaloclastite

[45] In samples from 1087.3, 1106.7, 1225.9, 1299.7, 1308, and 1334.76 mbsl, some pore-lining smectite cement is present, forming isopachous coatings of smectite (i.e., pore-lining, marginal layers of more or less constant thickness) a few micrometers thick and spherulitic masses on the order of 15 to 20 μm in diameter (Figure 1). Some shards and other grains have fractured. Congruent dissolution is noticable, but not abundant. Side-

romelane in hyaloclastites from the zone of incipient alteration is not visibly altered to palagonite. On the other hand, red-brown smectitic grain replacement with tubules is widespread, though never pervasive or complete. Qualitative, summary reactions for this zone could be written as

Sideromelane + additional constituents

$= $ pore $-$ lining smectite 1 $+$ apatite

$+$ dissolved constituents,

Sideromelane $=$ secondary pores $+$ titaniferous nodules

$+$ dissolved constituents,

and

Sideromelane $+$ additional constituents

$=$ reddened, smectitic grain $-$ replacement

$+$ titaniferous nodules $+$ apatite $+$ dissolved constituents.

[46] These reactions occur in approximately the order indicated.

4.3. Smectitic Alteration

[47] In a zone that lies below the zone of incipiently altered hyaloclastite and is 200 m or less thick, the predominant pattern of alteration is formation of smectite as isopachous layers and spherulites, pore-filling cements, and fillings of dissolved shards (Figure 1). Our samples from depths of 1403.6 mbsl, 1478.5 mbsl, and 1566.7 mbsl display smectitic alteration. The sample from 1573.6 mbsl displays smectitic alteration overprinted by palagonitic alteration. In vesicular shards, the occurrence and texture of minerals within some of the vesicles resembles that in the pores; other vesicles have no alteration or have a variation of the normal pattern of alteration described below. As stated above, samples collected from the zone of smectitic alteration retain the alteration features described for the zone of incipient alteration.

[48] Smectite occurs in a variety of settings in the zone of smectitic alteration. It fills ghosts of shards in which smectite 1 coatings or iron hydroxide stains mark primary external boundaries and vesicles; it fills many primary pores, and it fills the spaces left by dissolving of olivine grains (Figure 4c). Smectites in all three pore-filling situations resemble pore-lining smectite 2 in color and birefringence, but they lack the consistent optical orientation of that constituent. A microprobe analysis from this zone (Table 2, sample from 1426 m) indicates that this is one of the most aluminous and iron-rich smectites from the HSDP hyaloclastites.

[49] Alteration of olivine is more extensive in thin sections displaying smectitic alteration than in either of the zones of incipient alteration or normal alteration (Figure 4c). Most olivine grains are at least partially altered to smectite in these samples, in contrast to samples from other alteration zones of hyaloclastites in the core. In dissolved olivine grains, smectite may appear in well-oriented domains that mimic the cracks formed by the natural parting of olivine or the exterior margin of the grain. Some grains display markedly etched boundaries. Plagioclase and pyroxenes are not affected by alteration.

[50] Dissolved shards and smectite pseudomorphs of shards are more common in samples from the zone of smectitic alteration than they are in samples from other alteration zones (Figure 4c). They contain the titaniferous nodules characteristic of dissolved shards, secondary pores, and reddened smectitic grain replacement in the zone of incipient alteration.

[51] We have not resolved whether smectite replacement of shards is a passive filling of secondary pores or a direct replacement of glass by smectite. Optical resemblance between smectite filling primary pores and that in pseudomorphs of shards does suggest that the smectite grew into a void created by solution of the shard, rather than directly replacing the glass. However, microprobe analyses show that while grain-replacing smectite 2 is generally close in composition to that of other forms of smectite, it consistently contains higher concentrations of Ti than corresponding smectite in primary pores (cf. smectite analyses from 1426 m in Tables 2 and 3). This suggests replacement of sideromelane and "inheritance" of aspects of composition.

[52] While the major feature of smectitic alteration is formation of pore-filling smectite and smectite replacements of glass and olivine, phillipsite is an important constituent of all samples from this zone. Phillipsite forms spherulitic masses of prismatic crystals in pores of samples that display smectitic alteration.

[53] Qualitative summary alteration reactions for the zone of smectitic alteration would be

Sideromelane + added constituents

$\quad$ = pore − lining or pore − filling smectite 2

$\quad\quad$ + green smectitic grain replacement

$\quad\quad$ + titaniferous nodules + apatite

$\quad\quad$ + dissolved constituents.

Sideromelane + added constituents = phillipsite + Ca

$\quad$ − silicate + dissolved constituents.

$\quad\quad\quad$ And

Olivine + added constituents = smectite

$\quad\quad\quad\quad$ + dissolved constituents.

[54] Formation of phillipsite overlaps both formation of pore-lining smectite 2 and the subsequent

formation of Ca-silicate in time. The temporal relationship of the olivine dissolution and replacement relative to the other reactions is not resolved.

4.4. Palagonitic Alteration

[55] In hyaloclastite samples from 1573.6 m to the deepest hyaloclastite samples we examined, from below 2900 m, virtually all sideromelane grains in the HSDP core are marginally altered to palagonite (Figure 1). This generalization applies to shards in apparently massive hyaloclastites, traction- or suspension-bedded hyaloclastites, and sideromelane debris accumulated in spaces between basalt pillows. It applies to primary surfaces of fragments, vesicle margins, glass adjacent to fractures that cut across shards, and fragments of crushed shards. Chabazite fills pore spaces in hyaloclastite that were not earlier completely filled with isopachous or spheroidal layers of smectite or radiating masses of phillipsite and diaphanous masses of Ca-silicate.

[56] The smectite and phillipsite are carryovers from earlier stages of alteration, as are fracturing, tubules, green or reddened grain replacements, and areas of dissolved sideromelane that are spotted with titanite nodules and, in the zone of palagonitic alteration, more or less filled with chabazite. Interestingly, only the uppermost sample from the zone of palagonitic alteration shows evidence of smectitic alteration. Palagonitic alteration is thus rarely overprinted on earlier kinds of alteration, and represents a progressive development from incipient alteration, but only exceptionally from the more extensive smectite-forming processes of smectitic alteration.

[57] The characteristic reaction of palagonitic alteration is

$$\text{Sideromelane} + \text{added constituents} = \text{palagonite} + \text{chabazite}$$
$$+ \text{dissolved constituents.}$$
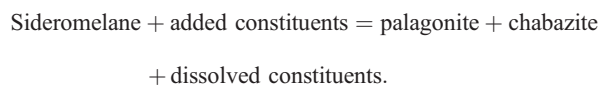
4.5. Conditions of Alteration

[58] The modern hydrologic framework, water geochemistry, and temperature regime of the HDSP boring are not necessarily those at which alteration took place. However, the history of the area is relatively simple and modern conditions represent a point in the evolution from the initial conditions. As such, they may provide some insight into the conditions of alteration. The boundary between the subaerial portion of the core and the portion that accumulated below sea level is at 1080 mbsl, implying subsidence of over a kilometer since the accumulation built above sea level at about 450 Ka (D. DePaolo and W. Sharp, Age-depth relations in the HSDP-2 Core, document circulated to HSDP participants, 10/01, 2001). There is no reported interfingering of submarine and subaerial deposits [*DePaolo et al.*, 2000]. It is doubtful that submarine deposits spent long periods above sea level or in an unsaturated zone of the hydrologic system. All alteration textures are consistent with a system of solids and pore fluids, without air bubbles in the center of pores.

[59] Salinity history of the groundwaters is more problematic; glacioeustatic changes of sea level may have changed the hydrologic regime, by shifting the elevation of the freshwater-saltwater interface in the subsurface. Meteoric water may have circulated to considerable depth in the area of the boring (D. Thomas, personal communication, 2002). The effects of sea level change and meteoric invasion of the system remain to be elucidated. Studies of the hydrology of the HSDP 2 area and chemistry of the recovered waters are still in progress.

[60] Logs indicate that downhole temperature declines with depth from the surface to about 800 m, where it is some 9°C [*Thomas*, 2000]. From this depth T increases, but at a relatively low rate, reaching about 45°C at the bottom of the hole. At the top of the submarine section, the modern temperature in the zone of initial alteration is 12° to 15°C. The boundary between smectitic alteration and palagonitic alteration lies at about 200 m below the base of the zone of initial alteration is just over 15°C. While these temperature measurements may not indicate alteration temperatures, they suggest that the thermal gradient was low, and temperature increase was probably not the only factor in promoting different outcomes of alteration. Moreover, the alteration mineralogy, particularly the zeolites phillipsite and chabazite,

implies that paleotemperatures in the borehole are unlikely to have been significantly greater then present-day temperatures.

4.6. Timing of Alteration

[61] Palagonitic alteration, characteristically the reaction of sideromelane to produce gel palagonite and chabazite, apparently took place in a narrow zone. The lack of change of porosity downward through the zone of palagonitic alteration and the lack of increase of thickness of gel palagonite rinds (Figures 10 and 16) imply that palagonitization and the growth of chabazite represent a brief stage in the history of each sample, a thin zone of reaction. The top of that reaction zone now lies at ~1570 m depth, at a temperature of just over 15°C. The reaction occurs as the rocks enter that zone, perhaps passing a critical chemical or thermal threshold as they reach the top of the zone of palagonitic alteration. The reaction then ceases, as it is limited by reduced permeability (implied by the low porosity), by saturation of the chemical system or by depletion of the available water. The top of the zone of palagonitic alteration also closely coincides with the marked decrease in water absorption in HSDP 2 Phase 1 core samples [*Moore*, 2001]. Moore suggested that this change reflects reduction of permeability due to increased cementation. Rising temperatures to the bottom of the hole have not significantly increased the amount of palagonite, changed the mineralogy of the samples, or affected the porosity of samples.

[62] If characteristic features of palagonitic alteration formed in a narrow zone, they probably did so quickly. Overall burial rates for the submarine portion of the core are of the order of 18 m/Ka [*DePaolo and Sharp*, 2001]. If palagonite and chabazite form progressively through a zone 100 m thick, the formation of gel palagonite rinds about 0.1 mm thick must take 5 to 6 Ka, the length of time it takes for the samples to pass through that zone. The temperature in that zone today is about 15°C. This rate of formation at that temperature (~0.02 μm/year) is in the range indicated by *Moore* [1966] and *Jakobsson and Moore* [1986] for palagonite growth.

5. Discussion: Comparison With Previous Studies

[63] Most previous reports concerning palagonite have been based on a small number of samples from a few outcrops or dredge hauls [e.g., *Peacock*, 1926; *Melson and Thompson*, 1973; *Eggleton and Keller*, 1982; *Furnes*, 1984; *Thorseth et al.*, 1991; *Le Gal et al.*, 1999], or from shallow cores into oceanic sediments or basement [e.g., *Scarfe and Smith*, 1977; *Andrews*, 1977; *Ailin-Pyzik and Sommer*, 1981; *Zhou and Fyfe*, 1989]. Few of these investigators had the benefit of the wealth of information available from the HSDP-2 project: (1) the age and history of the system, (2) the potential for inferring pore water composition, (3) constraints on temperatures, and (4) a view of the process at various stages of development because of nearly continuous core recovery. Even the extensive studies of *Hay and Iijima* [1968a, 1968b], *Honnorez* [1978, 1981], and *Kristmannsdottir and Thomasson* [1978] do not provide a stepwise view of the transition over distances measured in tens to hundreds of meters.

5.1. Comparison to Other Palagonite-Forming Alteration Systems

[64] The HSDP samples from the zone of palagonitic alteration most closely match an initial stage of alteration as defined by *Honnorez* [1978, 1981] who differentiated between initial, mature, and final stages of palagonitization as delineated by textural and mineralogical criteria. In Honnorez's initial stage, only pores are filled with secondary minerals (including smectite, gyrolite, and phillipsite), and cores of unaltered glass are rimmed with palagonite. In the HSDP samples from the zone of palagonitic alteration, the margins of large glass grains and all of the small ones are altered to palagonite, smectite lines all pores, and the remaining intergranular pores, fracture voids, and vesicles are virtually filled with phillipsite, Ca-silicates, and chabazite. The progression of pore-filling minerals is also similar between the two systems. *Honnorez* [1978] reported a progression of smectite, gyrolite, phillipsite and then chabazite, with some alternation of smectite and gyrolite. In HSDP samples, we

observe temporal alternation between phillipsite and smectite and between phillipsite and Ca-silicates, but a smectite is clearly the first phase to form in pores and chabazite is last.

[65] In the HSDP samples, however, the extended depth range of the sample suite allows differentiation that is not possible in single or small exposures. We can define additional stages of alteration and show that formation of each mineral or variety of each mineral is limited in time in the history of the sample. Pore-lining smectite 1 assigned to the incipient phase of alteration does not intergrow with any later minerals. Furthermore, different reactions define stages of this alteration, as described above. Formation of palagonite and of chabazite are simultaneous but occur after the formation of pore lining smectite 2, phillipsite, and Ca-silicates, which interfinger in time. Finally, the HSDP system shows varieties of grain replacement that precede *Honnorez*'s [1978, 1981] initial stage of palagonitization, rather than following it.

[66] In this respect, HSDP samples bear some resemblance to the fracture-focused oxidative alteration and palagonitic alteration initially described by *Andrews* [1977]. He interpreted the fracture-focused alteration as accompanying the percolation of oxidizing seawater through oceanic basalts. However, Andrews interpreted this palagonitic alteration as having occurred during or just after emplacement of basalts, rather than post-dating some incipient phase of alteration, as we do here.

[67] *Hay and Iijima* [1968a, 1968b] stressed the importance of pH in controlling the conversion of sideromelane to palagonite versus pedogenic clays in tephras from the Honolulu Group of Oahu. In soil zones and in wet climates, cation leaching and de-silication are the dominant weathering processes, and basalt glass alters to a variety of pedogenic clays including kaolinite and halloysite, but not to palagonite and zeolites [*Schiffman et al.*, 2000, 2003]. Hydrolysis of basaltic glass within sideromelane-rich tephras leads to increasing pH. When pH rises above 9 to 9.5, the solubility of aluminum (as aluminate ion) and silica (as dissociated silicic acid) both increase, but the solubility of zeolites does not, resulting in precipitation of

zeolites as opposed to smectites [*Mariner and Surdam*, 1970].

[68] These observations may help explain the changes from incipient to palagonitic alteration in the HSPD core that occur despite the minor changes in alteration temperature inferred from modern values. Pore fluids in the HSDP hyaloclastites at depths equivalent to the smectitic/palagonitic zone boundary, may have reached a high enough value of pH to leave the stability field of smectite and enter that of zeolites. Petrography actually suggests that conditions were in the vicinity of coexistence of phillipsite and smectite for some period of time, before progressing through the phillipsite and Ca-silicate field into the chabazite field.

5.2. Smectitic Alteration

[69] Smectitic alteration superficially resembles the Honnorez's mature stage of alteration marked by virtually complete conversion of original sideromelane to residual altered glass or palagonite. In Honnorez's mature stage, phillipsite (with minor smectite) has begun to replace the shards, but the hyaloclastite texture remains visible. In the HSDP hyaloclastites, pores are entirely filled with smectite and zeolites, chiefly phillipsite. Palagonite replaces the margins of shards, but not the interior of large shards. Green, smectitic grain replacement affects the margins of some shards. However, several key differences exist between Honnorez's mature stage and the HSDP zone of smectitic alteration. In the HSDP hyaloclastites, the grain-replacing material is primarily smectite, not zeolite, and titaniferous spherules are another major component of the replacing material. In addition, olivine is marginally etched and replaced by smectite rather than being essentially fresh. Finally, smectitic alteration predates formation of characteristic features of the zone of palagonitic alteration, rather than following them. The characteristic minerals are earlier in the succession. Chabazite that is coeval with the formation of palagonite margins on shards forms later than phillipsite. The zone of smectitic alteration lies above the zone of palagonite alteration and below the zone of incipient alteration. Palagonite appears to loop around areas

of smectitic replacement rather than being cross-cut by it, as though the palagonitization altered the margin of unaltered glass after partial replacement by smectite and associated phases. Palagonite margins on shards formed after the smectitic grain replacement, not before it.

5.3. Comparison to Other Systems Showing Reddened Smectitic Grain-Replacements

[70] In a study of altered basaltic glasses from archeological sites in Hawaii, *Morgenstein and Riley* [1975] reported that the boundary between altered glass (palagonite in their terms) and fresh glass consisted of a "microfracture-chemical channel zone which may be considered the mist zone of the glass" and an insoluble product layer. The number of microfractures increased from the inner edge of the mist zone outwards to the insoluble product layer. In their view, hydration of the basaltic glass had proceeded along the mist zone, as components were dissolved and subsequently accumulated to form the insoluble product layer. The resulting palagonite is banded, marking the repeated incremental progress of the process of forming the mist zone, the insoluble product layer, and the subsequent replacement of both with palagonite.

[71] On re-examination, the plates in *Morgenstein and Riley* [1975] appear to show tubules, not fractures in the mist zone. These features lie at different planes of focus, and do not extend all the way through the thickness of the thin section. They appear to cross, they curve up and down in the thin section, and where they emerge at its surface, they are seen to be elliptical in cross-section, as though they are oblique cuts of a round tube. Petrographic and SEM examination of mist zones in HSDP samples show they consist of numerous tubules that extend inward from the edge of remaining glass (Figures 4a, 4b, 7, and 8).

[72] The significance of mist zones, insoluble product layers, and microtubules in the palagonitization of oceanic basalts has been noted by *Melson and Thompson* [1973], who argued that alteration of MORB alkalic basalts occurred through a fringe of microtubules in the glass, and by *Staudigel and*

Hart [1983], who drew on the existence of the mist zone in their discussion of the formation of palagonite. Palagonite from DSDP site 335 displays a dendritic pattern of alteration of glass that is remarkably like textures found in some HSDP hyaloclastites that display reddened smectitic replacement of glass. *Zhou and Fyfe* [1989] described dendritic alteration as extending into fresh glass from its margin, and forming a boundary between the glass and two distinct forms of alteration they call palagonite. Outward from the center of shards, the progression is fresh sideromelane, dendritic alteration, a dark brown, translucent, non-isotropic, homogeneous band they call gel palagonite and an orange or yellow layer of finely laminated alteration they call fibrous palagonite. Their fibrous palagonite is laminated and birefringent. Although the dendritic pattern of alteration in the DSDP samples is markedly similar to that observed in the HSDP samples (cf. Figure 4b with *Zhou and Fyfe* [1989, Figure 1]), they differ in that the dendritic pattern is not present in many of the HSDP samples displaying palagonitic alteration but is present in HSDP samples from both the incipient and smectitic zones of alteration.

[73] Like the tubules, dendritic alteration is not part of the process of forming palagonite (in the sense we use it here) in HSDP samples. However, many HSDP samples display tubules (mist zones), insoluble product layers, dendritic patterns of glass replacement and reddened grain-replacing smectites (Figure 1). These are all present in samples from our zones of incipient and smectitic alteration, with the features progressively more developed with increasing depth in samples from the zone of incipient alteration. Samples we have described as displaying palagonitic alteration may have such zones, but not at the boundary between palagonite (as defined here) and sideromelane. Instead, palagonitization has occurred around or engulfing mist zones, as though it occurred later, rather than being truncated by them, as would imply an earlier formation. Tubules may extend across the rind of palagonite or may terminate in it. In HSDP samples, a characteristic assemblage includes the mist zone-immobile product layer-reddened smectitic grain replacement as a characteristic feature of

the early stage of alteration, but these features are unrelated to growth of palagonite later in the alteration history.

5.4. Microbial Origin of Mist Zones

[74] Understanding of the formation of mist zones in alteration of sideromelane has taken a substantial advance with the suggestion that they are the result of microbial activity [*Thorseth et al.*, 1992; *Staudigel et al.*, 1995; *Thorseth et al.*, 1995a, 1995b; *Torsvik et al.*, 1998; *Fisk et al.*, 1998]. *Thorseth et al.* [1992] showed that microbes exist on the surface of fresh basaltic glass and, through their metabolic activity, form distinctive pit-like or sponge-like textures. *Thorseth et al.* [1995a, 1995b], *Giovannoni et al.* [1996], *Furnes et al.* [1996], and *Torsvik et al.* [1998] used stains and genetic probes to demonstrate strong associations of DNA with vermiform, tubular, or spherical structures and to mark specific kinds of organisms. *Fisk et al.* [1998] described at least eight styles of pits, channels, tunnels, and voids that formed as a result of microbial weathering.

[75] Our own interpretation of the trinity of mist zones, insoluble product layers, and reddened smectitic grain replacement is that the tubules in the mist zones are the result of microbial activity. Several observations support this conclusion. The tubules in the HSDP hyaloclastites curve and closely resemble tubules in altered basaltic glass photographed by *Thorseth et al.* [1995b], *Furnes et al.* [1996], *Fisk et al.* [1998] or described by *Torsvik et al.* [1998]. In the HSDP core, these features are not homogeneously distributed along grain margins. Instead their occurrence is spotty, as though communities of organisms formed and grew at specific points, or the entire surface was colonized but conditions were somewhat more favorable for organic growth at certain points (similar to the "discrete microcolonies" of *Thorseth et al.* [1992]). Finally, thin sections with petrographically visible tubules take DAPI stains (Figure 8) [c.f. *Thorseth et al.*, 1995b; *Torsvik et al.*, 1998]. We also suggest that the "rooted zones", which are so similar to those of *Zhou and Fyfe* [1989] are either of organic origin or reflect dissolution of

glass promoted by increased surface area that is caused by organic activity.

6. Conclusion: Multiple Styles and Sequential Alteration of Basalt Glass in the HSDP Core

[76] Hyaloclastites from the HSPD 2 Phase 1 core allow for a comprehensive study of the stages and processes of alteration of sideromelane. Observations summarized here show that basalt glass in hyaloclastites of that core has altered by at least four different processes: dissolution, biological attack producing reddened smectitic grain replacements, a (presumably abiotic) process producing green smectitic grain replacements, and the formation of palagonite. Future work will describe the distinctive effects of contact metamorphism on hyaloclastites in the core. All of these processes have left characteristic petrographic evidence of their occurrence and timing.

[77] The incipient stage of alteration involved fracturing and formation of smectite pore linings on all surfaces. Dissolution of some shards leaves primary crystals unaffected, but produces titaniferous nodules.

[78] Microbes colonized shard surfaces, fractures, and vesicles in the early stages of alteration. Their activities lead to formation of the mist zone or tubules. Tubules, which are trace fossils, are associated with the insoluble product layer, and reddened smectitic grain replacement, including titaniferous nodules and apatite.

[79] During the stage of smectitic alteration, smectite filled pores and, with titaniferous nodules, replaced hyaloclastite shards. Smectite also replaced olivine. In samples showing smectitic replacement, features of the incipient stage of alteration are also present. Spheroidal phillipsite and a second generation of pore-lining smectite alternate times of their formation, followed by growth of Ca-silicates and more phillipsite.

[80] During the stage of palagonitic alteration, palagonite replaced the margins of hyaloclastite shards and chabazite filled remaining pore space, overprinting previous alteration patterns. In the

HSDP hyaloclastites, the timing of palagonitization as well as the chemical composition of palagonite implies that it is not - as others have previously suggested - an intermediary step in the evolution of sideromelane to smectite.

[81] The conditions of formation of the various alteration minerals in the HSDP hyaloclastites products are imperfectly known. The lack of change of porosity and thickness of palagonite rinds downward through the zone of palagonitic alteration suggests palagonite and chabazite formed in a narrow zone. Today, the boundaries between the zones of alteration (incipient, smectitic, and palagonitic) lie in a narrow range from $\sim 12°$ to $\sim 15°C$. If those temperatures prevailed during alteration, it is likely that vital effects or chemical thresholds were important in differentiating the outcomes.

[82] Clearly, alteration of hyaloclastites has occurred in a series of steps and produced a variety of different outcomes. At any one location in the core, one reaction or set of reactions characterized the alteration process at any time, but different reactions occurred previously or subsequently. On the basis of this series of reactions, it is possible to examine the mass balance of the alteration process of hyaloclastites and the mobility of elements in the suboceanic-island environment.

Acknowledgments

References

Ailin-Pyzik, I. B., and S. E. Sommer, Microscale chemical effects of low temperature alteration of DSDP basaltic glasses, *J. Geophys. Res.*, *86*, 9503–9510, 1981.

Andrews, A. J., Low temperature fluid alteration of oceanic layer 2 basalts, DSDP Leg 37, *Can. J. Earth Sci.*, *14*, 911–926, 1977.

DePaolo, D. J., D. M. Thomas, E. M. Stolper, and M. O. Garcia, Scientific Drilling Project: Core logs and summarizing data, rep., Calif. Inst. of Technol., Pasadena, 2000.

Eggleton, R. A., and J. Keller, The palagonitization of limburgite glass: A TEM study, *Neues. Jahrb. Mineral.*, *7*, 321–336, 1982.

Fisher, R. V., and H-U Schmincke, *Pyroclastic Rocks*, Springer-Verlag, New York, 1984.

Fisk, M. R., S. J. Giovannoni, and I. H. Thorseth, Alteration of oceanic volcanic glass: Textural evidence of microbial activity, *Science*, *281*, 978–980, 1998.

Furnes, H., Chemical changes during progressive subaerial palagonitization of a subglacial olivine tholeiite hyaloclastite; a microprobe study, *Chem. Geol.*, *43*, 271–285, 1984.

Furnes, H., I. H. Thorseth, O. Tumyr, T. Torsvik, and M. R. Fisk, Microbial activity in the alteration of glass from pillow lavas from hole 896A, *Proc. Ocean Drill. Program Sci. Results*, *148*, 191–206, 1996.

Giovannoni, S. J., M. R. Fisk, T. D. Mullins, and H. Furnes, Genetic evidence for endolithic microbial life colonizing basaltic glass/seawater interfaces, *Proc. Ocean Drill. Program Sci. Results*, *148*, 207–214, 1996.

Hay, R. L., and A. Iijima, Nature and origin of palagonite tuffs of the Honolulu Group on Oahu, Hawaii, in *Studies in Volcanology: A Memoir in Honor of Howel Williams*, pp. 331–376, Geol. Soc. of Am., Boulder, Colo., 1968a.

Hay, R. L., and A. Iijima, Petrology of palagonite tuffs of Koko Craters, Oahu, Hawaii, *Cont. Mineral. Petrol.*, *17*, 141–154, 1968b.

Honnorez, J., Generation of phillipsites by palagonitization of basaltic glass in sea water and the origin of K-rich deep-sea deposits: *Natural Zeolites Occurrence, Properties, Use*, edited by L. B. Sand and F. A. Mumpton, pp. 245–258, Pergamon, New York, 1978.

Honnorez, J., The aging of the oceanic lithosphere, in *The Oceanic Lithosphere*, edited by C. Emiliani, pp. 525–587, John Wiley, New York, 1981.

Jakobsson, S. P., and J. G. Moore, Hydrothermal minerals and alteration rates at Surtsey volcano, Iceland, *Geol Soc. Am. Bull.*, *97*, 648–659, 1986.

Jercinovic, M. J., K. Keil, M. R. Smith, and R. A. Schmitt, Alteration of basaltic glasses from north-central British Columbia, Canada, *Geochim Cosmochim Acta*, *54*, 2679–2696, 1990.

Kristmannsdottir, H., and J. Thomasson, Zeolite zones in geothermal areas in Iceland, *Natural Zeolites Occurrence, Properties, Use*, edited by L. B. Sand and F. A. Mumpton, pp. 277–284, Pergamon, New York, 1978.

Le Gal, X., J. L. Crovisier, F. Gauthier-Lafaye, J. Honnorez, and B. Grambow, Meteoric alteration of Icelandic volcanic glass: long term changes in the mechanism, *C.R. Acad. Sci., Ser. IIa Sci. Terre Planetes*, *329*, 175–181, 1999.

Mariner, R. H., and R. C. Surdam, Alkalinity and formation of zeolites in saline alkaline lakes, *Science*, *170*, 977–980, 1970.

Melson, W. G., and G. Thompson, Glassy abyssal basalts, Atlantic sea floor near St Paul's Rocks: Petrography and composition of secondary clay minerals, *Geol. Soc. Am. Bull.*, *84*, 703–716, 1973.

Moore, J. G., Rate of palagonitization of submarine basalt adjacent to Hawaii, *U.S. Geol. Surv. Prof. Pap.*, *550-D*, D163–D171, 1966.

Moore, J. G., Density of basalt core from Hilo drill hole, Hawaii, *J. Volcanol. Geotherm. Res.*, *112*, 221–230, 2001.

Morgenstein, M., and T. J. Riley, Hydration rind dating of basaltic glass: A new method for archeological chronologies, *Asian Perspect.*, *17*, 154–159, 1975.

Peacock, M. A., The petrology of Iceland, Part 1, The basic tuffs, *Trans. R. Soc. Edinburgh Earth Sci.*, *55*, 53–75, 1926.

Pryor, W. A., Permeability and porosity variations in some Holocene sand bodies, *Am. Assoc. Petrol. Geol. Bull.*, *60*, 162–189, 1973.

Scarfe, C. M., and D. G. W. Smith, Secondary minerals in some basaltic rocks from DSDP Leg 37, *Can. J. Earth Sci.*, *14*, 903–910, 1977.

Schiffman, P., H. J. Spero, R. J. Southard, and D. A. Swanson, Controls on palaonitization versus pedogenic weathering of basaltic tephra: Evidence from the consolidation and geochemistry of the Keanakako'I Ash Member, Kilauea Volcano, *Geochem. Geophys. Geosyst.*, *1*, Paper number 2000GC000068, 2000.

Schiffman, P., R. J. Southard, D. D. Eberl, and J. L. Bishop, Distinguishing palagonitized from pedogenically-altered basaltic Hawaiian tephra: Mineralogic and geochemical criteria, in *Volcano -Ice Interactions on Earth and Mars*, edited by J. L. Smellie and M. G. Chapman, *Geol. Soc. Spec. Publ.*, *202*, 393–405, 2003.

Singer, A., and A. Banin, Characteristics and mode of formation of palagonite—A review, *Proc. Int. Clay Conf.*, *9*, 173–181, 1990.

Staudigel, H., and S. R. Hart, Alteration of basaltic glass: Mechanisms and significance for the ocean-seawater budget, *Geochim. Cosmochim. Acta*, *47*, 337–350, 1983.

Staudigel, H., R. A. Chastain, A. Yayanos, and W. Bourcier, Biologically mediated dissolution of glass, *Chem. Geol.*, *126*, 147–154, 1995.

Stroncik, N. A., and H.-U. Schmincke, Evolution of palagonite: Crystallization, chemical changes, element budget, *Geochem. Geophys. Geosyst.*, *2*, Paper number 2000GC000102, 2001.

Thomas, D., Hydrologic conditions within Mauna Kea volcano, *Eos Trans. AGU*, *81*(48), Fall Meet. Suppl., 2000.

Thorseth, I. H., H. Furnes, and O. Tumyr, A textural and chemical study of Icelandic palagonite of varied composition and its bearing on the mechanism of the glass-palagonite transformation, *Geochim. Cosmochim. Acta*, *55*, 731–749, 1991.

Thorseth, I. H., H. Furnes, and M. Heldal, The importance of microbiological activity in the alteration of natural basaltic glass, *Geochim. Cosmochim. Acta*, *56*, 845–850, 1992.

Thorseth, I. H., H. Furnes, and O. Tumyr, Textural and chemical effects of bacterial activity on basaltic glass: an experimental approach, *Chem. Geol.*, *119*, 139–160, 1995a.

Thorseth, I. H., T. Torsvik, H. Furnes, and K. Muehlenbachs, Microbes play an important role in the alteration of oceanic crust, *Chem. Geol.*, *126*, 137–146, 1995b.

Torsvik, T., H. Furnes, K. Muehlenbachs, I. H. Thorseth, and O. Tumyr, Evidence for microbial activity at the glass-alteration interface in oceanic basalts, *Earth Planet. Sci. Lett.*, *162*, 165–176, 1998.

van der Plas, L., and A. C. Tobi, A chart for judging the reliability of point counting results, *Am. J. Sci.*, *263*, 87–90, 1965.

von Waltershausen, W. S., Über die submarinen Ausbrüche in der tertiären Formation des Val di Noto im Vergleich mit verwandten Erscheinungen am Åtna, *Gött. Stud.*, *1*, 371–431, 1845.

Walton, A. W., P. Schiffman, and G. Macpherson, Mass balance attending gel palagonitization in the HSDP-2 Phase 1 core, *Eos Trans. AGU*, *83*(47), Fall Meet. Suppl., F1499, 2002.

Yu, W., W. K. Dodds, K. Banks, J. Skalsky, and E. A. Strauss, Optimal staining and sample storage time for direct microscopic enumeration of total and active bacteria in soil with two fluorescent dyes, *Appl. Environ. Microbiol.*, *61*, 3367–3372, 1995.

Zhou, Z., and W. S. Fyfe, Palagonitization of basaltic glass from DSDP Site 335, Leg 37: Textures, chemical composition, and mechanism of formation, *Am. Mineral.*, *74*, 1045–1053, 1989.

Zhou, Z., W. S. Fyfe, K. Tazaki, and S. J. Vandergaast, The structural characteristics of palagonite from DSDP Site 335, *Can. Mineral.*, *30*, 75–81, 1992.